ARTICLE IN PRESS

Available online at www.sciencedirect.com

ScienceDirect

Solar Energy xxx (2014) xxx–xxx

SOLAR ENERGY

www.elsevier.com/locate/solener

Solar updraft tower power generation

Xinping Zhou *, Yangyang Xu

Department of Mechanics, Huazhong University of Science and Technology, Wuhan 430074, PR China

Received 26 January 2014; received in revised form 27 April 2014; accepted 22 June 2014

Communicated by: Associate Editor Yogi Goswami

Abstract

Solar updraft tower power generation has been demonstrated to be a promising approach for future applications of solar radiation to provide energy. In this paper, the history of the solar updraft tower power plant (SUTPP, also called solar chimney power plant) technology is reviewed, its characteristics are presented, and its principle is described. The experimental studies, main important factors of theoretical modelings, and cost studies, in the past few decades, are reviewed. The characteristics of novel non-conventional SUTPP technologies are discussed as well as environmental effect and power production conditions for the SUTPP technology.

Keywords: Solar updraft tower; Solar collector; Turbine; Power generation

1. Introduction

1.1. History

Solar updraft tower power plant (SUTPP, also called solar chimney power plant, Fig. 1) is a kind of device that produces buoyancy to drive air to ascend for electricity generation (Schlaich, 1995). The concept of using a small SUT device for furnishing power first appeared in Bennett (1896)'s patent, and a household SUT device for generating electricity was proposed in a magazine by Cabanyes (1903). In 1926, Dubos proposed the construction of an SUTPP in North Africa with its tower on the slope of a high mountain (Ley, 1954). The SUTPP concept was later described in a publication by Günther (1931). Lucier (1978, 1979a, 1979b, 1981) had a more complete design of an SUTPP, and his patents on SUTPP were granted in Canada, Australia, Israel, and the USA, respectively.

Schlaich together with his colleagues built the first pilot SUTPP prototype in Manzanares, Spain in 1982 (Haaf et al., 1983; Haaf, 1984). The pilot prototype had an SUT 194.6 m high and a collector 122 m in radius. The prototype operated with a peak power of about 50 kW for seven years from 1983 to 1989 (Schlaich, 1995). The successful operation of the prototype demonstrated the feasibility and reliability of the SUTPP technology. Since then, many researchers have shown strong interest in it and extensively studied the potential of SUTPP technology all over the world (Zhou et al., 2010b). In order to generate electricity economically, a large-area collector and a high SUT are needed for an SUTPP. Some commercial SUTPP projects have since been proposed in several countries (Table 1). However, until now, this technology has not yet been commercialized.

1.2. Description

A conventional SUTPP (Fig. 1) consists of a circular solar collector constructed on horizontal ground, a vertical

* Corresponding author. Tel.: +86 27 87543838; fax: +86 27 87542221.
E-mail address: xpzhou08@hust.edu.cn (X. Zhou).

http://dx.doi.org/10.1016/j.solener.2014.06.029
0038-092X/

Nomenclature

A	area (m^2)
b	thermal effusivity ($W\ s^{1/2}/K\ m^2$)
C	cost (€)
c_p	specific heat capacity (J/kg K)
D	diameter (m)
d_h	hydraulic diameter (m)
F	force (N/m)
f	Darcy friction factor
g	gravitational acceleration, 9.81 (m/s^2)
H	height (m)
h	heat transfer coefficient (W/m^2 K)
i	interest rate (%)
inf	inflation rate (%)
k	thermal conductivity (W/m K)
m	pressure potential exponent
$\dot{m}$	mass flow rate (kg/s)
N	length of service life (year)
Nu	Nusselt number
n	pressure loss exponent
P	power (W) or electricity (kW h)
Pr	Prandtl number
p	pressure (Pa)
q	heat flux (W/m^2)
R	specific gas constant of air (J/kg K)
Re	Reynolds number
r	radius (m)
S	global solar radiation (W/m^2)
T	temperature (K)
t	time (s)
V	volume flow rate (m^3/s)
v	velocity (m/s)
x	turbine pressure drop factor
z	depth in ground or height above ground (m)

Greek symbols

α	thermal diffusivity (m^2/s)
β	volumetric thermal expansion coefficient of air (1/K)
γ	specific heat ratio
Δ	difference
η	efficiency (%)
θ	angle (radian)
μ	dynamic viscosity (kg/m s)
ρ	density (kg/m^3)
τ	shear stress (Pa)
φ	effective absorption coefficient of collector
ψ	roof heat loss coefficient (W/m^2 K)

Subscripts

a	ambient air
avg	average
b	ground at a considerable depth
$coll$	collector
f	air flow
$force$	forced convection
g	ground
h	horizontal surface
ii	initial investment
nat	natural convection
$no\ turb$	without turbine
om	operation and maintenance
p	absorber surface
pb	absorber surface into ground
pf	absorber surface to airflow
$poten$	potential
pr	absorber surface to roof
r	roof
ra	roof to ambient air
rf	roof to airflow
rin	compression rings
rs	roof to sky
s	sky
sup	supports
sut	solar updraft tower
tg	turbine generators
$turb$	turbine
$turb,i$	turbine inlet
w	wind
1	surroundings on ground level
2	collector inlet
3	collector outlet
4	turbine inlet
5	turbine outlet
6	SUT outlet
7	atmosphere at the height of SUT outlet

solid SUT situated at the center of the collector, and turbine generators installed at the collector outlet or at the SUT inlet (Schlaich, 1995). In the solar collector, solar radiation passes through the transparent roof and is received by the absorber, i.e., the ground or an additional absorber laid on the ground, and thus the indoor air is heated. Some heat is stored in the absorber when solar radiation is strong during day time on sunny days. The heat is released from the absorber when solar radiation is weak during night time or on cloudy days. The density difference between the warm air inside the SUT and the ambient air creates buoyancy that acts as the driving force and is also called pressure potential. The buoyancy drives the air to flow in the collector toward the SUT base and rise in the SUT. Finally, the air current drives the turbines powering generators to generate electricity.

Please cite this article in press as: Zhou, X., Xu, Y. Solar updraft tower power generation. Sol. Energy (2014), http://dx.doi.org/10.1016/j.solener.2014.06.029

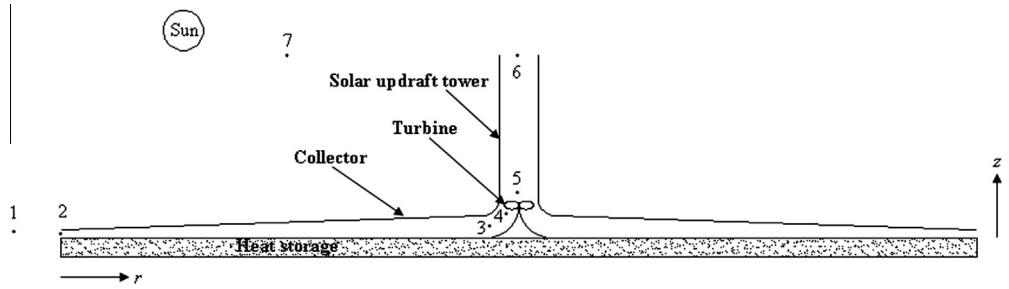

Fig. 1. Schematic of a conventional solar updraft tower power plant (1: surroundings on ground level, 2: collector inlet, 3: collector outlet, 4: turbine inlet, 5: turbine outlet, 6: SUT outlet, 7: atmosphere at the height of SUT outlet).

Table 1
Several selected commercial SUTPP proposals.

Power capacity (MW)	SUT height (km)	Collector area (km^2)	Location	References
200[a]	1	38.5	Mildura/Australia	Zhou et al. (2010b) and Wikipedia (2014)
40[b]	0.75	3.5	Ciudad Real/Spain	Zhou et al. (2010b) and Wikipedia (2014)
400[c]	1.5	37	Namibia	Zhou et al. (2010b) and Wikipedia (2014)
–	1	–	Shanghai/China	Zhou et al. (2010b)
27.5[d]	–	2.77	Wuhai/China	Wikipedia (2014)
–[e]	1	–	Near Meekatharra/Australia	Evans (2011)
200[f]	About 0.8	Over 12.7	Arizona/USA	Spencer (2013)

[a] Proposed in 2001.
[b] Planned to be completed by 2010.
[c] Proposed in 2008.
[d] It consists of three phases covering a total area of 277 hectares and its total power capacity is expected to reach 27.5 MW. The first phase to build the Wuhai pilot prototype was completed in 2010, and the final phase was planned to be completed by 2013.
[e] In 2011, Hyperion Energy planned to build the SUTPP to supply power to Mid-West mining projects.
[f] It was reported in June 2013 that EnviroMission was progressing through the permitting process and planned to start construction of the project in late 2014.

A solar collector consists of support columns, a framework matrix, and a transparent roof made of glass, plastic or other transparent materials. An air collector is formed when the transparent roof is suspended from the framework matrix supported above the ground by the support columns. The roof of a typical collector slowly ascends from the collector periphery to its center to guide indoor airflow with low friction losses.

Natural ground has a certain heat storage capacity, but its heat storage capacity cannot always meet the need of SUTPP operation during night time or on cloudy days. Therefore, additional heat storage systems have been proposed to help store solar energy. Since water with large specific heat capacity is a kind of cheap and effective heat storage medium, a water-filled system placed on the ground under the collector roof has been regarded as a typical additional heat storage system (Kreetz, 1997; Schlaich et al., 2005). The water-filled system is closed and airtight to avoid heat loss by evaporation.

The SUT situated at the center of the collector is the thermal engine of the SUTPP. The best choice for high SUT structure has been considered by civil engineers (Schlaich, 1995; Krätzig et al., 2009) to be reinforced concrete shell structure due to its long life span and favorable cost amongst many possible structural designs, although a guyed corrugated metal sheet flue was designed by Schlaich and his colleagues for the Manzanares prototype just for experimental purposes. Civil engineers (Schlaich, 1999; Krätzig et al., 2009; Harte et al., 2013) designed high ring-stiffened thin-walled reinforced concrete cylindrical or hyperbolic shell SUTs for commercial SUTPPs.

Turbines are driven by the air current due to buoyancy to transfer fluid power to shaft power (Fluri and von Backström, 2008a). The typical SUT turbine is of the axial flow type, whose characteristics (e.g., the number of rotor blades) lie between those of wind turbine and gas turbine. Its blades are adjustable like those of wind turbine, but the air flow is enclosed just as in gas turbine, and the SUT turbine may have inlet guide vanes (IGVs) (Von Backström and Gannon, 2004). The SUT supports could be used as IGVs of the single vertical-axis turbine installed at the SUT base (Gannon and von Backström, 2003). Turbine configuration is the single vertical-axis, the multiple vertical-axis or the multiple horizontal-axis type (Schlaich, 1995). Turbine layout is the single-rotor layout (Gannon and von Backström, 2003), or the counter-rotating layout with one pair of counter-rotating rotors (Denantes and Bilgen, 2006), both with or without IGVs.

1.3. General characteristics

SUTPP is one of the promising renewable energy-based power suppliers on a large scale and can be suitably located in arid and semi-arid zones and remote regions (Zhou

et al., 2013c). In general, commercial application of SUTPP has the following advantages:

(1) The technology is simple. The construction materials, mainly steel, concrete and glass, are widely available. Construction sites may be desert areas. It is accessible to almost any countries including the technologically less developed countries.
(2) The solar collector absorbs direct and diffuse solar radiation. The SUTPP with the natural-additional mixed heat storage system can operate day and night on pure solar energy. This is crucial to the development of SUTPPs in tropical regions where the weather is frequently overcast.
(3) Its operation and maintenance expense is relatively low. Although turbine maintenances and sporadically collector cleaning are costly, additional fossil fuels are not required to substitute solar radiation due to reliable operation of SUTPP day and night. Cooling water is also not required during SUTPP operation. The moving or rotating parts are few other than turbine blades and this would lead to few occurrences of mechanical failures and high safety.
(4) Its global warming potential is low for the entire life cycle including construction, operation and decommissioning phases (Zongker, 2013). It is nearly pollution free during operation. It uses renewable energy source: solar radiation, and its operation avoids the emissions of large amounts of greenhouse gases and the use of potable water for cooling purposes.
(5) Its power output and efficiency increase with its dimension, and the energy production cost is reduced (Schlaich et al., 2004; Krätzig, 2013). Carbon credit revenue due to carbon emission reduction can improve its cost effectiveness (Fluri et al., 2009; Li et al., 2014).

Therefore, commercial SUTPPs producing electric power with almost no pollution can make the most of abundant solar radiation on vast desert areas. The power produced from commercial SUTPPs is thought to be a good alternative to that from fossil fuels. However, there are also some disadvantages of SUTPPs:

(1) The investment is huge for the construction of a commercial plant due to the cost of its large-area collector and high SUT. The commercial SUTPP construction demands huge amounts of construction materials. Although cooling water is not needed, large quantities of water may be required to work as a medium of additional heat storage.
(2) Its efficiency is low due to the several-process energy conversions and small temperature difference between the hot and cold reservoirs. (The efficiency for a large-scale plant, however, can reach to an acceptable level. Levelized electricity cost (LEC) is actually a more important indicator to determine the economic feasibility of building an SUTPP than the plant investment and efficiency (Schlaich et al., 2004; Krätzig, 2013).)
(3) Its SUT height is limited. The reinforced concrete SUT is required to be as high as possible in order to improve the plant efficiency. However, because of the technological constraints and the restrictions on the construction materials, it is difficult to construct a very high SUT. There are also external limitations such as possible earthquakes, which may destroy high SUT.
(4) Environmental concerns may arise. Construction and operation of many commercial SUTPPs may influence the local environment, ecology, and then lives of different plant and animal species.

These disadvantages put obstacles in the way of the commercialization of the SUTPP technology.

2. Principle of operation

The energy conversion processes related to SUTPP can be demonstrated with a temperature-entropy diagram of air standard cycle analysis without considering system losses (Gannon and Von Backström, 2000) as shown in Fig. 2. In the figure, the collector inlet area is assumed to be large enough, resulting in a small velocity of airflow at the collector inlet, and the velocity of airflow at Point 3 is assumed to be equal to that at Point 4. Process 2–3 occurring in the collector denotes that the air entering through the collector inlet from the surroundings is heated by solar radiation, its temperature and entropy increase, and the indoor air motion is accelerated, while the total pressure is kept constant inside the collector. Process 4–5 denotes that the air blows through the turbine into the SUT when the temperature and static pressure decrease slightly. This is seen as an isentropic process. Process 5–6 denotes that the air behind the turbine flows through the SUT when the temperature decreases mainly due to the negative work done by the gravitational force. This is also seen as an isentropic process. Process 6–7 denotes that the energy including kinetic energy and heat of airflow is released into the atmosphere. In the following sections,

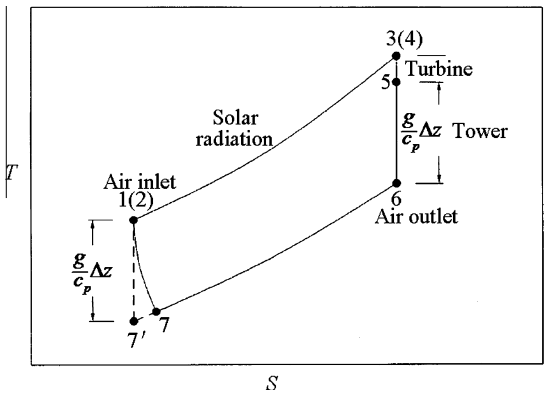

Fig. 2. Temperature-entropy diagram of air standard cycle without system losses for SUTPP (Gannon and von Backström, 2000).

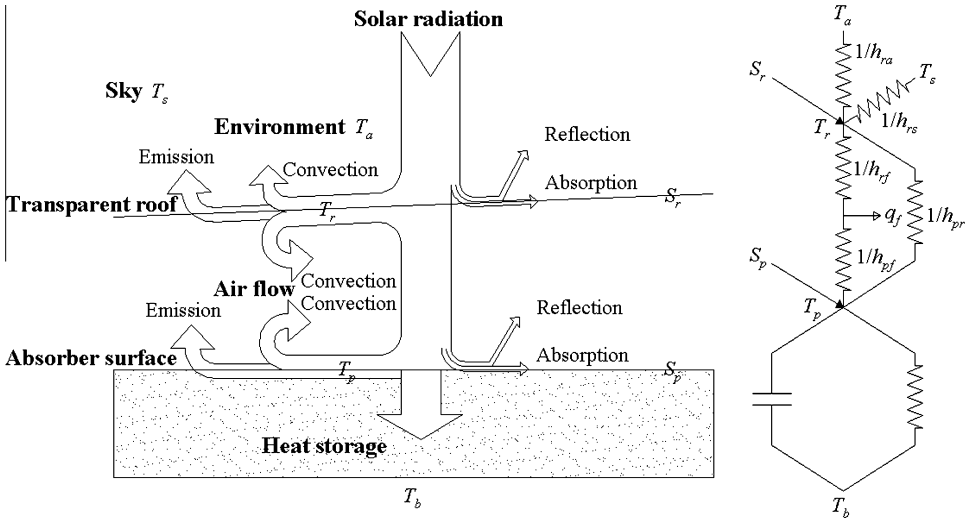

Fig. 3. Heat transfer scheme of a conventional SUTPP collector with natural ground heat storage system.

energy conversion processes related to the main components of the conventional SUTPP, i.e., solar collector, heat storage, SUT, and turbines, are discussed in detail by considering the system losses.

2.1. Solar collector

Heat transfer scheme in a conventional solar collector with natural ground heat storage system is presented in Fig. 3. The transparent roof of the solar collector admits direct and diffuse solar radiation and retains long-wave radiation from the ground. This produces greenhouse effect in the collector. The ground under the roof heats up and transfers its heat to the airflow above it.

The conventional SUTPP is axisymmetric. Besides, as compared to the collector diameter of several thousand meters for a commercial SUTPP, the roof height is very low. The air flow and heat transfer in the SUTPP collector can be numerically simulated by solving the relevant equations of a one-dimensional compressible flow in the radial direction. The air is regarded as an ideal gas with its density ρ calculated using the state equation:

$$\rho = \frac{p}{RT} \tag{1}$$

where p, R, and T denote the static pressure, the gas constant, and the temperature of the air, respectively. Relatively slow changes in the airflow dynamics in the collector induce the transient terms in the relevant equations to be negligible (Pretorius, 2004, 2007). The continuity equation for variable roof height along the radius is written as

$$\frac{d}{dr}(\rho v r H) = 0 \tag{2}$$

where v denotes the velocity of the airflow at radius r, while H is the roof height above the absorber surface. The momentum equation in the radial direction is therefore,

$$\rho v H \frac{dv}{dr} = -H\frac{dp}{dr} + \left(\tau_r + \tau_p + \frac{F_{\text{sup}}}{r\Delta\theta}\right) \tag{3}$$

where τ_r is the roof shear stress, τ_p is the absorber shear stress, and F_{sup} is the drag force exerted by the supports of the roof. Air energy balance is represented by

$$q_{rf} + q_{pf} = -c_p \rho v H \frac{dT}{dr} \tag{4}$$

where q_{rf} and q_{pf} are the convective heat flux from the roof and the absorber surface to the airflow, respectively, and c_p is the specific heat capacity of air and can be assumed to be constant at small temperature range of the air, whereas the roof and ground surface energy balances are given by Eqs. (5) and (6) respectively.

$$S_r + q_{pr} = q_{ra} + q_{rs} + q_{rf} \tag{5}$$

where S_r is the global solar radiation absorbed by the collector roof, q_{ra} is the convective heat flux from the roof to the environment mainly due to ambient winds, and q_{pr} and q_{rs} are the radiative heat flux from the absorber surface to the roof and from the roof to the sky, respectively, and

$$S_p = q_{pr} + q_{pf} + q_{pb} \tag{6}$$

where S_p is the global solar radiation absorbed by the absorber, and q_{pb} is the heat flux from the absorber surface into the ground at a considerable depth.

In the solar collector, the heat gains from solar radiation are used to heat and raise the indoor air and accelerate the air motion. As compared to the heat gains of the airflow, the increases in the gravitational potential energy of the air and the fluid power of the airflow inside the collector are negligible. In this case, the thermal efficiency of the solar collector, η_{coll}, can be approximated as

$$\eta_{coll} = \frac{c_p \dot{m}(T_3 - T_2)}{A_{coll} S_h} \tag{7}$$

Please cite this article in press as: Zhou, X., Xu, Y. Solar updraft tower power generation. Sol. Energy (2014), http://dx.doi.org/10.1016/j.solener.2014.06.029

where $\dot{m}$ is the mass flow rate of air inside the SUTPP, A_{coll} is the collector area, and S_h is the global solar radiation on a horizontal surface.

2.2. Heat storage

The two main heat storage systems for SUTPPs are the natural ground system and the typical natural-additional mixed system with a closed water-filled system. The former is more convenient and cheaper but has worse heat storage capacity than the latter. Different heat storage mechanisms for SUTPP have been used in various mathematical models. They are summarized in Table 2.

The heat transfer process in the natural ground heat storage system has been considered as conduction by many researchers. Because of axisymmetric body of the solar collector, the heat conduction in the circumferential direction in the heat storage system is negligible. Besides, the heat conduction in the radial direction is much weaker than that in the vertical direction. The transient heat conduction in the heat storage system can approximately be described by the reduced one-dimensional Fourier–Biot diffusion equation in the radial direction (Pretorius and Kröger, 2006b; Bernardes and Zhou, 2013a):

$$\frac{1}{\alpha_g}\frac{\partial T_g}{\partial t} = \frac{\partial^2 T_g}{\partial z^2} \tag{8}$$

where the ground thermal diffusivity α_g is defined as $\alpha_g = \frac{k_g}{\rho_g c_{pg}}$. The following boundary conditions are valid for Eq. (8): The heat flux from the ground surface ($z = 0$)

Table 2
Summary of SUTPP heat storage mechanisms in different mathematical models.

References	Mechanism	Thermal diffusivity directions	Flow or not	Thermal resistance below water layer or not
Ming et al. (2008a, 2013a), Zheng et al. (2010) and Xu et al. (2011)	Natural, porous	Vertical and radial[a]	Airflow	–
Haaf et al (1983), Pasumarthi and Sherif (1998a), Hedderwick (2001), Kröger and Buys (2002), Pretorius (2004), Pretorius (2007)[b], Pretorius and Kröger (2006b), Bernardes (2013), Gholamalizadeh and Mansouri (2013) and Xu et al. (2014)	Natural, non-porous	Vertical	No	–
Pastohr et al. (2004), Sangi et al. (2011) and Hurtado et al. (2012)[c], Asnaghi and Ladjevardi (2012) and Asnaghi et al. (2013)	Natural, non-porous	Vertical and radial[a]	No	–
Guo et al. (2013, 2014) and Gholamalizadeh and Kim (2014)	Natural, non-porous	Vertical, radial and circumferential[a]	No	–
Kreetz (1997)[d], Bernardes et al. (2003)[e] and Schlaich et al. (2005)[d]	Mixed, non-porous	Vertical	Convection in water	Yes
Papageorgiou (2006)[f] and Pretorius (2007)[b]	Water	–	–	Yes, thermal insulation
Bernardes and Zhou (2013a)[g]	Mixed, non-porous	Vertical	Convection in water producing vertical thermal stratification	Both cases: with and without thermal resistance
Ming et al. (2013c)[h]	Mixed, non-porous	Vertical and radial	No	No

[a] The heat transfer of the heat storage system in two directions was considered in a two-dimensional axisymmetric model using the commercial computational fluid dynamics (CFD) packages while the heat transfer in three directions was considered in three-dimensional model using CFD packages.

[b] The heat storage performance of various kinds of ground was studied, and the heat storage capacity of water tanks was also investigated. Each water tank was covered by a thin transparent plastic film, and its inner bottom surface was black. The bottom and sides of the water tank were assumed to be thermally insulated and a bulk mean water temperature was assumed.

[c] The ground was modeled as a solid material with a varying-with-depth bulk density and a varying-with-depth effective thermal conductivity, which were used to describe the ground porosity approximately without the air flow in the ground considered.

[d] The water tubes (or bags) were black. Their black top surfaces would absorb solar radiation in form of heat, transfer the heat downward and store the heat in the water and ground.

[e] In each water bag, the water lay between an upper transparent film and a bottom absorber. The upper transparent plastic film admits solar radiation, while the bottom absorber absorbs solar radiation.

[f] The water layer was used as the only heat storage medium in floating SUT power plant by excluding the heat storage of the ground. A bulk mean water temperature was assumed.

[g] In each water bag, the water lay between an upper transparent film and a bottom plastic film with good absorptivity. The vertical thermal stratification in the water bags was considered, which results from the natural convection driven by the thermal buoyancy because of the temperature difference between cold and hot water. In order to model the vertical thermal stratification caused by the natural convection in the water bags, the temperature calculated based on the assumption of the heat conduction process and no heat convection in water for each water sub-layer was sorted in a temperature-descending order in each time step.

[h] A water pool for heat storage was covered by a thin transparent plastic film. The heat was absorbed at each water sub-layer by an exponential decline with depth in water.

Please cite this article in press as: Zhou, X., Xu, Y. Solar updraft tower power generation. Sol. Energy (2014), http://dx.doi.org/10.1016/j.solener.2014.06.029

into the ground q_{pb} is equal to $-k_g \left.\frac{\partial T_g}{\partial z}\right|_{z=0}$, and at a considerable depth z_b the temperature gradient $\left.\frac{\partial T_g}{\partial z}\right|_{z=z_b}$ equals zero. The ground heat storage capacity depends on the ground thermal effusivity defined as $b_g = \sqrt{\rho_g c_{pg} k_g}$. A larger thermal effusivity of the ground leads to a better heat storage capacity and thus produces a more uniform profile of the SUTPP power output (Pretorius, 2007; Pretorius and Kröger, 2007). More compacted ground having larger thermal effusivity is therefore more beneficial for the SUTPP heat storage capacity. This is in agreement with CFD simulations carried out by Hurtado et al. (2012).

The air flow in the ground regarded as porous media has been considered in addition by a few researchers in CFD simulations of SUTPP (Ming et al., 2008a, 2013a; Zheng et al., 2010; Xu et al., 2011). CFD simulations showed that the air flow in the porous media is helpful in improving the heat transfer performance in the ground (Ming et al., 2008a). However, the density and the effective specific heat capacity due to the consideration of the porosity become smaller. The effect of the air flow in the porous media to the SUTPP heat storage capacity cannot be concluded from the definition of the ground thermal effusivity and the previous studies involving the air flow in the porous media for the SUTPP.

Different mixed heat storage systems with additional closed water-filled systems have been designed, and different heat storage mechanisms have been proposed. These are shown in Table 2. The special issue is vertical thermal stratification in the water bags (Bernardes and Zhou 2013a). The thermal stratification is caused by thermal buoyancy because of the temperature difference between cold and hot water. The thermal stratification produces higher temperatures in the upper layer of the water bags, and influences the heat transfer to air flow as well as the heat storage in ground. In order to evaluate the heat storage capacity of the water-filled systems, researchers have made comparisons between the daily power output profile for an SUTPP with water storage and that without water storage. Table 3 presents the proportions of the daily peak and valley power outputs of SUTPPs with water storage for several representative depths to the peak output without water storage, which are obtained from existing literature. The predictions are not uniform, which may be attributed mainly to the use of different heat storage mechanisms related to water. However, all the predictions returned good dynamic control of power output by using closed water-filled system because of the good heat storage capacity of water. Bernardes and Zhou (2013a) evaluated the SUTPP heat storage capacity by the efficiency of heat storage system, which was defined as the ratio of the heat extracted from the storage to the heat stored into it. The efficiency of the heat storage system with 0.2 m thick water bags in which vertical thermal stratification was considered can reach higher than 0.97, which is higher than the efficiency of 0.89 for the same plant without water bags.

2.3. Solar updraft tower

Various SUT shapes have been proposed. The conventional SUT for power generation is a cylinder where the cross sectional area almost does not change with height (Schlaich, 1995, 1999; Pretorius and Kröger, 2006b). The flow area in the SUT was proposed by von Backström and Gannon (2000a) to increase gradually with height from the SUT inlet to its outlet by 14% to keep the through-flow Mach number constant in order to eliminate the pressure drop associated with the vertical acceleration of the indoor air that is about three times the pressure drop associated with wall friction. The lower part of SUT was proposed to be hyperboloid like cooling tower in order to give benefits of shape strengthening (Borri et al., 2010; Harte et al., 2012). A convergent SUT was designed and built by Pasumarthi and Sherif (1998a, 1998b). It was indicated from the simple analytical model developed by Padki and Sherif (1999) that when the turbine was installed at the SUT outlet, the convergent SUT was helpful to increase the plant power output not by increasing the mass flow rate of the updraft in the SUT but by increasing the updraft velocity at the SUT outlet. A divergent SUT, together with other three cylindrical SUTs, was designed and built by Koonsrisuk (2009). The experimental data showed that divergent SUT helped increase the mass flow rate of air in the SUTPP (Koonsrisuk, 2009). CFD simulations showed that SUT shape influenced the performance of SUTs (Koonsrisuk and Chitsomboon, 2013b; Ming et al., 2013a; Putkaradze et al., 2013). Later, Patel et al. (2014) found the optimum divergent angle of 2° for a divergent SUT by using CFD simulations.

Relevant conservation equations for continuity, momentum, and air energy have been derived for a one-dimensional compressible flow in the vertical direction in an elementary control volume for variable SUT cross-sectional area with height (Von Backström and Gannon, 2000a; Von Backström, 2003). The equations are suitable for various-shaped SUTs. The continuity equation is written as

$$\frac{\mathrm{d}}{\mathrm{d}z}(\rho v A_{sut}) = 0 \tag{9}$$

where the SUT cross-sectional area A_{sut} is a function of height z that is assumed to increase from the ground ($z = 0$) to the SUT outlet ($z = H_{sut}$ where H_{sut} is the SUT height). The momentum equation without the inclusion of the buoyancy force is expressed as

$$\rho v \frac{\mathrm{d}v}{\mathrm{d}z} = -\frac{\mathrm{d}p}{\mathrm{d}z} - \left(\frac{4\tau_{sut}}{D_{sut}} + \frac{F_{\mathrm{rin}}}{A_{sut}}\right) - \rho g \tag{10}$$

while the momentum equation with the buoyancy force is

$$\rho v \frac{\mathrm{d}v}{\mathrm{d}z} = -\frac{\mathrm{d}p}{\mathrm{d}z} - \left(\frac{4\tau_{sut}}{D_{sut}} + \frac{F_{rin}}{A_{sut}}\right) - (\rho - \rho_a) g \tag{11}$$

where D_{sut} is the SUT diameter, ρ_a is the density of the ambient air, and F_{rin} is the drag force per unit SUT height

Please cite this article in press as: Zhou, X., Xu, Y. Solar updraft tower power generation. Sol. Energy (2014), http://dx.doi.org/10.1016/j.solener.2014.06.029

Table 3
Proportions of daily plant peak and valley power outputs with water storage to peak output without water storage.

References	Water storage thickness (m)	Proportion of valley with water to peak without water storage(%)	Proportion of peak with water to peak without water storage(%)
Kreetz (1997) and Schlaich et al. (2005)	0.1	22.7[a]	51.1[a]
	0.2	27.7[a]	43.9[a]
Bernardes et al. (2003)	0.1	12[b]	74[b]
	0.15	12.9[a]	73.9[a]
Papageorgiou (2006)[c]	0.125	39.4[a]	56.5[a]
	0.225	42.9[a]	55.2[a]
Pretorius (2007)	0.1	13	90
	0.2	30.9[a]	62.8[a]
Ming et al. (2013c)	0.1	32.7	69.0
	0.2	38.1[a]	64.9[a]

[a] Obtained from the figures in the references.
[b] Not reported in the reference but presented by Bernardes and Zhou (2013a).
[c] The heat storage capacity of the ground was assumed to be equivalent to that of a 2.5 cm thick water.

exerted by the evenly spaced internal spoked bracing wheels that are used to pre-stress the compression rings (Schlaich, 1999; Von Backström et al., 2008), or by the intrusive part of evenly spaced compression rings not pre-stressed by spoked wheels (Niemann et al., 2009), both of which are used to reinforce the high thin-walled shell SUT structures. The momentum equation of Eq. (10) is used with actual boundary conditions, that is, the total pressure at the inlet is specified as the ambient pressure on the ground level, and the static pressure at the SUT outlet is specified as the ambient pressure at its height. While, the pressure in the momentum equation of Eq. (11) should exclude the hydrostatic pressure variation due to ρ_a (ANSYS, 2012a). Therefore Eq. (11) is used with the assumed (impractical) boundary conditions, that is, both the total pressure at the SUT inlet and the static pressure at the SUT outlet are specified as the same value, which is always the local ambient pressure on the ground level. Because the energy losses of the updraft in the reinforced concrete SUTs are negligible, SUT air energy equation is given by

$$c_p \frac{dT}{dz} = -v\frac{dv}{dz} - g \tag{12}$$

The pressure potential of the SUTPP is in essence equal to the ambient atmospheric pressure difference between the collector inlet (Point 1) level and the SUT outlet (Point 7) level minus the gravitational force of the whole air inside the plant (Zhou et al., 2013d). It therefore can be given by (Schlaich, 1995):

$$\Delta p_{poten} = g\int_0^{H_{sut}} (\rho_a - \rho)dz \tag{13}$$

The energy conversion efficiency of the SUT can be defined as the proportion of the fluid power of the air current at the SUT inlet to the heat gains of the heated air current obtained from the solar collector. Schlaich (1995) presented a simplified form of the SUT efficiency:

$$\eta_{ch} = \frac{\dot{m}v_4^2/2}{c_p\dot{m}(T_3 - T_2)} = \frac{gH_{sut}}{c_pT_1} \tag{14}$$

where the velocity of air flow at the SUT inlet under no load condition, v_4, can be expressed as $v_4 = \sqrt{2gH_{sut}\frac{T_3-T_2}{T_1}}$ (Haaf et al., 1983; Schlaich, 1995; Padki and Sherif, 1999).

2.4. Turbine pressure drop

Most of the SUTPP pressure potential Δp_{poten} will be used at the turbine as static pressure, and the remaining will be used as the exit dynamic pressure and the system pressure losses (Von Backström and Gannon, 2000a; Pretorius and Kröger, 2006b). If all the pressure potential or no part of the pressure potential is used at the turbine as static pressure, no power will be produced from the SUTPP. The turbine pressure drop factor x is defined as the ratio of the turbine pressure drop Δp_{turb} to the plant pressure potential:

$$x = \Delta p_{turb}/\Delta p_{poten} \tag{15}$$

Under a turbine load condition, the static pressure and temperature of air behind the turbines can be given by

$$p_5 = p_1 - \Delta p_{coll} - \Delta p_{turb,i} - \Delta p_{turb} \tag{16}$$

$$T_5 = T_4 - \frac{\Delta p_{turb}V_{avg}}{c_p\dot{m}} \tag{17}$$

where $\Delta p_{turb,i}$ is the turbine inlet pressure loss, and V_{avg} is the average volume flow rate between Points 4 and 5. The average volume flow rate V_{avg} can be calculated with the average pressure and the average temperature between Points 4 and 5:

$$V_{avg} = \frac{\dot{m}}{\rho_{avg}} \tag{18}$$

where the average density ρ_{avg} is given by

$$\rho_{avg} = \frac{p_4 + p_5}{R(T_4 + T_5)} \tag{19}$$

2.5. Power output

The electric power extracted from the turbine generators under a turbine load condition, P, can be calculated by using the following equation (Pretorius and Kröger, 2006b; Zhou et al., 2014):

$$P = \eta_{tg}\Delta p_{turb}V_{avg} \tag{20}$$

where η_{tg} is the turbine generator efficiency, which is usually specified as a constant value. Selected values used in

Please cite this article in press as: Zhou, X., Xu, Y. Solar updraft tower power generation. Sol. Energy (2014), http://dx.doi.org/10.1016/j.solener.2014.06.029

Table 4
Selected values of turbine generator efficiency.

References	Value
Haaf et al. (1983)[a], Lodhi (1999), Kashiwa and Kashiwa (2008)[a] and Hurtado et al. (2012)[a]	83%
Schlaich (1995)[b]	77, 78.3, and 80.1%
Schlaich (1995)[b], von Backström and Gannon (2000b)[a], Dai et al. (2003)[a], Pretorius (2004, 2007), Pretorius and Kröger (2006a, 2006b, 2007, 2009), Nizetic et al. (2008), Fluri et al. (2009)[c], Bernardes et al. (2009), Zhou et al. (2009f, 2010c), Bernardes and von Backstrom (2010), Larbi et al. (2010)[a], Cao et al. (2011, 2013a, 2013c, 2014)[a], Cervone et al. (2011)[a], Xu et al. (2011)[a], Ming et al. (2013c) and Niroomand and Amidpour (2013)	80%
Bernardes et al. (2003)	75%
Zhou et al. (2007b)	50–90%
Bilgen and Rheault (2005)[a] and Zhou et al. (2013d, 2014)	77%
Ming et al. (2012)[d] and Ming et al. (2013b)[d]	72%

[a] The turbine efficiency in the references was actually used as the turbine generator efficiency.
[b] The values of 77%, 78.3%, and 80.1% were indicated for 5 MW, 30 MW, and 100 MW SUTPPs, respectively, in a table of this reference. Whereas, an approximate value of 80% was used for the 30 MW SUTPP in the appendix of this reference.
[c] Called the efficiency of the power conversion unit (PCU).
[d] The multiply of the turbine efficiency at about 0.8 and the generator efficiency at 0.9.

existing literature are shown in Table 4. In this model, the turbine generator efficiency is actually the total-to-total efficiency of the PCU. The PCU of a commercial SUTPP consists of one or several turbine generators, power electronics, a grid interface and the flow passage from collector outlet to SUT inlet. The assumption made by many other researchers that the turbine generator efficiency of a commercial SUTPP is 80% has been confirmed by Fluri and von Backström (2008b) using an analytical model. The SUTPP power output was also estimated conveniently by using the terms x and $\sqrt{1-x}$ to scale the pressure potential and the theoretical maximum volume flow rate at the SUT inlet under no load condition to obtain the turbine pressure drop and the volume flow rate at the SUT inlet respectively (Bernardes et al., 2003; Koonsrisuk and Chitsomboon, 2010) as $P = \eta_{tg}(x\Delta p_{poten,no\ turb})(\sqrt{1-x}V_{4,no\ turb})$. In this case, the pressure potential is independent of flow rate, and the maximum plant power is produced when the x value is 2/3. The power output estimated using the scaling method, however, was recently found significantly lower than that calculated using Eq. (20) under a turbine load condition, based on the assumed x value of 0.8 (Zhou et al., 2013d).

3. Important factors

Following the above introduction and analysis of the operation principle of SUTPP, it is seen that some factors are significant and can influence SUTPP performance to a large extent. Such factors for example, include the heat transfer coefficient, the turbine pressure drop factor, the pressure potential, the coefficients of the pressure losses in the SUT, and the turbine efficiency among others. In recent work on theoretical modelings and numerical simulations, different expressions or constants of some important factors (e.g., the heat transfer coefficient, the turbine pressure drop factor, and the pressure potential) have been used by different researchers. The expressions give rise to different results (e.g., Bernardes et al., 2009). All of the turbine inlet loss, the inside wall friction, the internal drag forces, the vertical acceleration of axial airflow, and the exit kinetic energy loss contribute to a pressure drop over the height of the SUT. The comprehensive work about the SUT pressure loss coefficients has been conducted by Von Backström and Gannon (2000a) and Von Backström et al. (2003). The SUT pressure losses also influence the turbine pressure drop factor. The comprehensive work about the turbine efficiency has been done by Fluri and von Backström (2008a, 2008b). In theoretical modelings and numerical simulations of SUTPP, the turbine generator efficiency is always assumed to be a constant, and various constants used in existing literature have been summarized in Table 4. Therefore, the work related to the SUT pressure loss coefficients and the turbine efficiency will not be discussed in this paper.

Other factors such as the air moisture and the ambient winds may, also influence SUTPP performance. In the following sections, discussions of the important factors of SUTPP used in literature are presented.

3.1. Heat transfer coefficient

With regard to the conventional SUTPP, there exist mainly radiative heat transfer from the collector roof to the sky and between the absorber and the roof, conductive heat transfer in the heat storage system, and convective heat transfer related to solar collector. The convective heat transfer behavior related to solar collector consists of two parts: the convective heat loss from the roof to the environment, and the convective heat transfer in the collector, i.e., between the ground and the indoor airflow, and between the roof and the indoor airflow. The correlations of the coefficients of the radiative and conductive heat transfer related to the collector have commonly been taken to be uniform in most previous studies. While, different mechanisms of convective heat transfer related to the collector have been considered, and different correlations have been used to calculate the convec-

Please cite this article in press as: Zhou, X., Xu, Y. Solar updraft tower power generation. Sol. Energy (2014), http://dx.doi.org/10.1016/j.solener.2014.06.029

Table 5
Summary of convective heat transfer mechanism from roof to environment and equations of heat transfer coefficient.

References	Mechanism	Condition	Equations for coefficient
Bernardes et al. (2003)	Natural convection	–	Based on Rayleigh number
Hedderwick (2001), Kröger and Buys (2001), Pretorius (2004), Larbi et al. (2010)[a], Asnaghi and Ladjevardi (2012)[a], Asnaghi et al. (2013)[a], Ming et al. (2013c) and Zou et al. (2014)	Forced convection	–	Using Eq. (21)
Pasumarthi and Sherif (1998a), Bilgen and Rheault (2005) and Zhou et al. (2010c)	Forced convection	–	Using Eq. (22)
Bernardes et al. (2009)	Mixed convection	–	Using Eq. (23)
Pretorius and Kröger (2006a)	Forced convection or mixed convection	–	Using Eq. (21) or Eq. (24)
Pretorius and Kröger (2006b), Pretorius (2007) and Bernardes and Zhou (2013b)	Forced or mixed convection	When $T_r > T_a$	Employing the higher of the values using Eqs. (24) and (25)
Pretorius and Kröger (2006b), Pretorius (2007) and Bernardes and Zhou (2013b)	Forced convection	When $T_a > T_r$	Using Eq. (25)
Zou et al. (2012, 2013)	Mixed convection	–	Using Eq. (24)
Gholamalizadeh and Kim (2014)	Forced convection	–	Using Eq. (25)

[a] They used an equation: $h = 5.67 + 3.86v_w$ where the constants approximate to those of Eq. (21).

tive heat transfer coefficients. In this section, the correlations of the convective heat transfer coefficients related to the collector, which determine the rates of the heat transfer between the roof and the environment, between the roof and the indoor airflow, and between the absorber and the indoor airflow, are summarized.

3.1.1. Convective heat transfer coefficient from roof to environment

Ambient winds will carry heat from the collector roof by convection. Different convective heat transfer mechanisms from the roof to the environment that have been used are shown in Table 5. Many researchers have regarded the convective heat loss from the roof to the environment as forced convective heat transfer other than Kröger's group and a minority of other researchers.

The temperature of the collector roof should be higher than that of the ambient winds during most of a day. Bernardes et al. (2003) therefore thought of the flow over the roof as a natural convection flow over a heated horizontal surface facing upward, and used common correlations based on Rayleigh number to calculate the natural convective heat transfer coefficient.

When ambient winds are strong and the temperature difference between the roof and the ambient winds is not significant, the forced convective heat transfer mechanism over the roof will dominate. Some previous studies about SUTPP (Hedderwick, 2001; Kröger and Buys, 2001; Pretorius, 2004; Larbi et al., 2010; Ming et al., 2013c) evaluated the forced convective heat transfer behavior from the collector roof to the environment by employing the following equation, which is based on Jurges's experimental data (Duffie and Beckman, 2013):

$$h = 5.7 + 3.8v_w \tag{21}$$

While other previous studies (Pasumarthi and Sherif, 1998a; Bilgen and Rheault, 2005; Zhou et al., 2010c) used another equation to determine the forced convective heat transfer coefficient to describe the heat transfer due to winds blowing over a roof surface (Duffie and Beckman, 2013):

$$h = 2.8 + 3v_w \tag{22}$$

Eq. (22) gives smaller value than Eq. (21) and was recommended by Watmuff et al. (1977) who suggested that Eq. (21) might include natural convection and radiation effects overestimating the forced convective heat transfer rate. The linear regression equations (including Eqs. (21) and (22)) of ambient wind-induced convective heat transfer from a flat plate to environment were effective in fitting the experimental data, even though fundamental heat transfer theory predicts a power relation between convective coefficient and ambient wind velocity (Palyvos, 2008). The convective heat transfer coefficient governed by either of Eqs. (21) and (22) is influenced only by ambient wind velocity. In this case, the mechanism of the ambient wind-induced convective heat transfer governed by either of Eqs. (21) and (22) is considered as forced convective heat transfer in this paper like in many references (e.g., Sharples and Charlesworth, 1998; Palyvos, 2008), though there is a constant heat transfer coefficient at no wind.

When both the forced convection due to the ambient winds and the natural convection take important effect, the flow may be seen as the mixture of a blown flow and a natural convection flow over a heated horizontal surface facing upward. Bernardes et al. (2009) used a natural-forced mixed convection correlation to calculate the coefficient of convective heat transfer over the roof under windy conditions:

$$\mathrm{Nu} = \left(\mathrm{Nu}_{\mathrm{force}}^3 + \mathrm{Nu}_{\mathrm{nat}}^3\right)^{1/3} \tag{23}$$

Whereas, Pretorius and Kröger (2006a, 2006b) used a mixed convection correlation during times when the collector roof temperature T_r exceeds the ambient temperature T_a, which was developed by Burger (2005) based on experimental data. The correlation is of the form:

$$h = \frac{0.2106 + 0.0026 v_w \left(\frac{\rho T_{avg}}{\mu g \Delta T}\right)^{1/3}}{\left(\frac{\mu T_{avg}}{g \Delta T c_p k^2 \rho^2}\right)^{1/3}} \quad (24)$$

where, T_{avg} is the average of the roof temperature T_r and the ambient temperature T_a. They also used another mixed convection correlation on any condition of whether or not T_r exceeds T_a, which was developed by Burger (2005) based on experimental data. The correlation is given by

$$h = 3.87 + 0.0022\left(\frac{v_w \rho c_p}{\mathrm{Pr}^{2/3}}\right) \quad (25)$$

The mechanism of the ambient wind-induced convective heat transfer governed by Eq. (25) is also considered as forced convective heat transfer for the same reason as those by Eqs. (21) and (22) in this paper.

3.1.2. Convective heat transfer coefficient in collector

Airflow is heated in the collector mainly by convection. The flow between the absorber and the roof in the collector may be regarded as having various flow conditions. Owing to a reasonable distance between the absorber surface and the collector roof, the flow in the collector has been regarded by many researchers as a flow involving two independent horizontal flat plates with the indefinitely and separately developed boundary layers (e.g., Bernardes et al., 2003; Pretorius and Kröger, 2006a, 2006b; Bernardes, 2011). The flow in the collector also may be seen as a flow in a channel between two infinite parallel plates (Pretorius and Kröger, 2006a, 2006b; Bernardes, 2011), or a flow between two finite stationary disks with converging flow developing (Bernardes, 2003, 2011).

Various mechanisms used to describe the convective heat transfer behavior in the collector are presented in Table 6. During most of a day, the mean temperature of the air inside the collector should be lower than that of the absorber surface and higher than that of the roof. Therefore, the flow in the collector was regarded as a natural convection flow. In the collector, the current driven by the SUT is in essence a blown flow. The flow in the collector was also regarded as forced convection flow. For example, Pretorius and Kröger (2006a, 2006b) used Gnielinski's equation to determine the coefficient of forced convective heat transfer including the effect of the specific surface roughness for fully developed turbulent flow between two parallel plates on the conditions of whether or not the roof temperature T_r and the absorber surface temperature T_p exceed the air flow temperature T:

Table 6
Summary of convective heat transfer mechanisms in collector (i.e. from absorber surface and roof to indoor air) and equations of heat transfer coefficients.

References	Mechanism	Condition	Equations for coefficients
Pasumarthi and Sherif (1998a), Bilgen and Rheault (2005), Bernardes et al. (2009)[a], Larbi et al. (2010), Bernardes (2011)[b], Cao et al. (2011) and Najmi et al. (2012)[c]	Natural convection	–	Based on Rayleigh number or Grashof number
Lodhi (1999), Kröger and Buys (1999, 2001, 2002)[d], Hedderwick (2001)[d], Bernardes et al. (2003), Bernardes et al. (2009)[a], Pretorius (2004)[e], Petela (2009), Bernardes (2011)[b], Ming et al. (2013c) and Najmi et al. (2012)[c]	Forced convection	–	Based on Reynolds number
Kreetz (1997), Pastohr et al. (2004), Sangi et al. (2011) and Niroomand and Amidpour (2013)	Mixed convection	–	Using Eq. (27)
Pretorius and Kröger (2006a)	Forced or mixed convection	When $T_p > T$ or $T_r < T$	Employing the higher of the values using Eqs. (24) and (26)
Pretorius and Kröger (2006a)	Forced convection	When $T_p < T$ or $T_r > T$	Using Eq. (26)
Pretorius and Kröger (2006b), Pretorius (2007) and Bernardes and Zhou (2013b)	Forced or mixed convection	When $T_p > T$ or $T_r < T$	Employing the highest of the values using Eqs. (24)–(26)
Pretorius and Kröger (2006b), Pretorius (2007) and Bernardes and Zhou (2013b)	Forced convection	When $T_p < T$ or $T_r > T$	Employing the higher of the values using Eqs. (25) and (26)
Zhou et al. (2009f), Li et al. (2012b), Zou et al. (2012, 2013) and Islamuddin et al. (2013)	Mixed convection	–	Using Eq. (24)
Gholamalizadeh and Mansouri (2013)[f]	Forced convection	–	Using Eq. (25), (26)

[a] Forced convection is general while natural convection becomes significant for low velocity flows.

[b] The flow in the collector was regarded as a forced, natural or mixed convection flow between two independent flat plates, or a forced or natural convection flow in a channel between infinite parallel plates, or a forced convection flow between two finite stationary disks with converging flow developing. Eqs. (24) and (25) were used for mixed convective heat transfer coefficients. The equation $\mathrm{Nu} = 230\left(\frac{2r}{D_{coll}}\right)^{0.65}\left(1 - \frac{2r}{D_{coll}}\right)^{-0.386}$ was recommended for calculating the local Nusselt number for thermally developing flow between two finite stationary disks, while the Nusselt number for thermally fully developed flow is given by: $\mathrm{Nu} \approx 2r/D_{coll}$ (Bernardes, 2003).

[c] The flow was regarded as forced convection flow when the roof was too low and as natural convection flow when the roof was too high.

[d] The coefficient applicable in the region of fully developed flow was different from that applicable in the region of developing flow.

[e] Using Eq. (26).

[f] Eq. (25) was used for calculating the convective heat transfer between the absorber surface and the indoor airflow though the equation was also claimed to be applicable for calculating the convective heat transfer between the roof and the indoor airflow. Whereas, Eq. (26) was used for calculating the convective heat transfer between the roof and the indoor airflow.

Please cite this article in press as: Zhou, X., Xu, Y. Solar updraft tower power generation. Sol. Energy (2014), http://dx.doi.org/10.1016/j.solener.2014.06.029

$$h = \frac{(f/8)(\mathrm{Re}-1000)\mathrm{Pr}}{1+12.7(f/8)^{1/2}(\mathrm{Pr}^{2/3}-1)}\left(\frac{k}{d_h}\right) \quad (26)$$

The flow in the collector was also seen as the mixture of a blown flow driven by SUT and a natural convection flow over a heated horizontal surface facing upward or a cooled horizontal surface facing downward. Kreetz (1997), Pastohr et al. (2004), Sangi et al. (2011), and Niroomand and Amidpour (2013) used the following correlation to calculate the mixed convective heat transfer coefficient:

$$\mathrm{Nu} = (\mathrm{Nu}_{\mathrm{force}}^4 + \mathrm{Nu}_{\mathrm{nat}}^4)^{1/4} \quad (27)$$

Pretorius and Kröger (2006b) used Eq. (24) to calculate the coefficient of mixed convective heat transfer from the absorber surface to the indoor air during times when T_p exceeds T, and to calculate the coefficient of mixed convective heat transfer from the roof to the indoor air during times when T exceeds T_r. They also used Eq. (25) on the conditions of whether or not T_p and T_r exceed T. Following Pretorius and Kröger (2006b), some researchers, e.g., Zhou et al. (2009f), Li et al. (2012b), Zou et al. (2012, 2013), Islamuddin et al. (2013), Gholamalizadeh and Mansouri (2013), and Bernardes and Zhou (2013b) employed one, two, or three of Eqs. (24)–(26) as basic equation(s) to describe the convective heat transfer behavior in the collector.

3.2. Pressure potential

The essential expression (Eq. (13)) of the SUTPP pressure potential is an integral form and inconvenient to use in the modeling calculations. Therefore, in most previous models, the essential expression is broken down and simplified for convenient calculation by assuming the air to be incompressible gas. The results will not be accurate enough due to the simplification.

Some previous studies (Mullett, 1987; Lodhi, 1999; Bilgen and Rheault, 2005; Cao et al., 2013a, 2013c) simplified the essential expression of the SUTPP pressure potential into the following form by assuming the density difference between the air inside the SUT and the ambient air not to change with height:

$$\Delta p_{poten} = (\rho_a - \rho) g H_{sut} \quad (28)$$

Based on the Boussinesq approximation, the SUTPP pressure potential can further be given by:

$$\Delta p_{poten} = \rho g \beta (T - T_a) H_{sut} \quad (29)$$

where β is the volumetric thermal expansion coefficient of air. The above equation was used by Koonsrisuk et al. (2010) and Lorente et al. (2010). A variation of Eq. (29) for estimating the SUTPP power potential was used by Schlaich (1995):

$$\Delta p_{poten} = \rho g H_{sut} \frac{T - T_a}{T_a} \quad (30)$$

Many previous studies (Haaf et al., 1983; Lodhi, 1999; Dai et al., 2003; von Backström and Fluri, 2006; Nizetic et al., 2008; Larbi et al., 2010; Bernardes and von Backstrom, 2010; Al-Dabbas, 2011b; Sangi, 2012; Buğutekin, 2012; Okoye and Atikol, 2014) also used Eq. (30) to estimate the SUTPP pressure potential. By substituting an empirical expression of air density with temperature within a small range into the essential expression (Eq. (13)) and employing the function of the temperatures with height, other simplified expressions were derived to estimate the SUTPP pressure potential (Zhou et al., 2009e, 2009f; Li et al., 2012b).

In order to reduce labor intensive programming and program debugging, some commercial CFD packages (mainly including Fluent and CFX) have been used by many researchers to simulate the air flow and heat transfer related to SUTPP by activating the built-in buoyancy models. A Boussinesq buoyancy model and a full buoyancy model can be activated in CFX (ANSYS, 2012a), whereas only the Boussinesq buoyancy model can be activated in Fluent (ANSYS, 2012b). Pastohr et al. (2004), Ming et al. (2008b, 2012, 2013a, 2013b), Zheng et al. (2010), Sangi et al. (2011), Al-Dabbas (2011b), Xu et al. (2011), Li et al. (2012a), Asnaghi and Ladjevardi (2012), Asnaghi et al. (2013), Guo et al. (2013, 2014), Xu et al. (2014), and Zou et al. (2014) simulated the air flow and heat transfer in SUTPP using the Boussinesq buoyancy model with FLUENT. Stamatov (2010) used the Boussinesq buoyancy model with the Finite Element Analysis Simulator, FEMLAB. Bernardes et al. (1999), Chergui et al. (2010) and Zandian and Ashjaee (2013) used the Boussinesq buoyancy model in their numerical simulations. Koonsrisuk and Chitsomboon (2007), Koonsrisuk and Chitsomboon (2009a, 2009b), and Patel et al. (2014) have done similar work using the full buoyancy model with CFX, whereas Maia et al. (2009a) used the full buoyancy model in their numerical simulations. In Boussinesq buoyancy model, the Boussinesq approximation is employed, and the buoyancy force is evaluated approximately from the difference between air temperature and a constant reference temperature based on an incompressible flow, while in full buoyancy model, the buoyancy force is evaluated directly from the difference between air density and a reference density, and the reference density is kept constant though the compressibility of air is considered. Neglecting the compressibility of the air inside or outside the SUT results in inaccuracy in the calculated results (Zhou et al., 2009d).

In order to ensure the accuracy of calculation, it is necessary to consider the compressibility of the air inside and outside SUT to estimate the SUTPP pressure potential. The SUTPP pressure potential is usually considered to be equal to the dynamic pressure at the SUT inlet under no load condition and is given by $\Delta p_{poten} = \frac{1}{2}\rho_5 v_5^2$. This is taken to be equal to the difference between the ambient pressure on the ground level and the static pressure at the SUT inlet under no load condition, that is, $\Delta p_{poten} = p_1 - p_5$. Based on this, Kröger and Blaine (1999) developed an expression

Table 7
Constants and expressions of optimal turbine pressure drop factor.

References	Constants and expressions
Pasumarthi and Sherif (1998a), Pastohr et al. (2004), Onyango and Ochieng (2006), Sangi et al. (2011), Asnaghi and Ladjevardi (2012) and Zandian and Ashjaee (2013)	16/27
Haaf et al. (1983), Lautenschlager et al. (1984), Mullett (1987), Schlaich (1995)[a], Lodhi (1999), von Backström and Gannon (2000b), Dai et al. (2003), Zhou et al. (2007b), Kashiwa and Kashiwa (2008), Petela (2009), Koonsrisuk and Chitsomboon (2010), Koonsrisuk and Chitsomboon (2013a), Larbi et al. (2010), Al-Dabbas (2011b), Hurtado et al. (2012), Sangi (2012), Fasel et al. (2013), Meng et al. (2013), Islamuddin et al. (2013) and Chen et al. (2014)	2/3
Schlaich (1995)[a]	0.82
Hedderwick (2001)	0.66–0.7
Bernardes et al. (2003)[b]	0.97
Schlaich et al. (2005), Zhou et al. (2013d, 2014) and Gholamalizadeh and Kim (2014)	0.8
Von Backström and Fluri (2006)[c]	$(n-m)/(n+1)$
Nizetic and Klarin (2010)[d]	$1-\frac{v_5^2 T_1}{2gH_{sut}}\left(\sqrt{\frac{\varphi}{\psi}\cdot S_h\cdot\frac{v_5^2 T_1}{2gH_{sut}}}\right)^{-1}$
Bernardes and von Backstrom (2010)[e]	Variable
Zhou et al. (2010a)	0.9
Li et al. (2012b)[f]	Variable
Guo et al. (2013)[g]	$1-\frac{m+1}{3}$
Ming et al. (2013c)	0.85
Koonsrisuk and Chitsomboon (2013a)[h]	Variable
Bernard es and Zhou (2013b)[i]	Variable

[a] An optimal value of 2/3 was obtained in the theoretical model of this reference, while a value of about 0.82 was calculated from the data for 5, 30, and 100 MW SUTPPs in a table of this reference.

[b] Bernardes et al. (2003) found an optimal value as high as approximately 0.97, but pointed out that this value was hard to achieve in reality, and recommended a value between 0.8 and 0.9. They selected a value of 0.9 in their model.

[c] m and n are the pressure potential exponent and the pressure loss exponent, respectively. m is typically a negative number between 0 and −1, and n is typically equal to 2. The optimal x value therefore changes from 2/3 for a constant pressure potential, independent of flow rate to approximately 1.

[d] φ is the effective absorption coefficient of the collector, and ψ is the roof heat loss coefficient. The optimal x values are in the range of 0.8–0.92 for various expected SUT inlet airflow velocities from 9 to 15 m/s and φ/ψ ratios from 0.09 to 0.18 for the Manzanares prototype.

[e] The optimal value remained around 0.9 during most of a day but could drop to 0.52.

[f] The optimal value calculated with the developed theoretical model increased from 0.825 for solar radiation of 500 W/m^2 to 0.855 for solar radiation of 1000 W/m^2 for the Manzanares prototype.

[g] The optimal values for the Manzanares prototype reached about 0.91, 0.92, 0.93, and 0.93 for solar radiation of 200, 400, 600, and 800 W/m^2 respectively using the developed theoretical model where m values were determined using CFD simulations. The values are slightly higher than those reaching about 0.91, 0.91, 0.89, and 0.88 using sole CFD simulations, respectively.

[h] The optimum value was equal to 2/3 for a constant pressure potential, and was a function of the plant size and solar heat flux for a non-constant pressure potential. The optimum value for the proposed Thai SUTPP with a collector radius of 200 m and an SUT height of 400 m was equal to 0.84 approximately.

[i] The optimal value remained around 0.8 during most of a day but could drop to about 0.2.

containing no integral for the pressure potential of the conventional SUTPP during relatively quiet (no significant ambient winds) periods by considering the dry air inside and outside the SUT as an ideal gas. The expression is of the form:

$$\Delta p_{poten} = p_1\left(1-\left(\frac{1-\frac{gH_{sut}}{c_pT_1}}{1-\frac{gH_{sut}}{c_pT_5}}\right)^{\gamma/(\gamma-1)}\right) \tag{31}$$

Eq. (31) has been proved to predict the SUTPP pressure potential as accurately as the essential expression of Eq. (13) could (Zhou et al., 2013d). Some researchers (Pretorius, 2004, 2007; Pretorius and Kröger, 2006b; Zhou et al., 2012, 2013d, 2014) have used the accurate expression to predict the SUTPP pressure potential in their models.

3.3. Turbine pressure drop factor

The pressure drop at the SUT turbine is very important for the power extracted from the turbine. The turbine pressure drop factor can significantly influence the SUTPP performance, and can be considered as an independent control variable of the SUTPP power output (Schlaich et al., 2005; Bernardes and von Backstrom, 2010; Bernardes and Zhou, 2013b; Guo et al., 2013). The optimal turbine pressure drop factor has been widely used conveniently for producing the maximum power from SUTPPs. By now, some constants and expressions of the optimal turbine pressure drop factor have been presented, which are summarized in Table 7.

The maximum possible power extracted from the turbine was considered by some researchers (Pasumarthi and Sherif, 1998a; Onyango and Ochieng, 2006; Zandian and Ashjaee, 2013) to be equal to the wind kinetic energy multiplied by the Betz's coefficient of 16/27. A few researchers (Pastohr et al., 2004; Sangi et al., 2011; Asnaghi and Ladjevardi, 2012) used the Betz's coefficient of 16/27 as the turbine pressure drop factor for calculating the maximum pressure jump at the turbine in their CFD simulations. Practically, only the wind turbine in an open wind farm follows the Betz limit. However, the airflow in the SUTPP is not an open flow, and the SUT turbines work

Please cite this article in press as: Zhou, X., Xu, Y. Solar updraft tower power generation. Sol. Energy (2014), http://dx.doi.org/10.1016/j.solener.2014.06.029

as shrouded pressure-staged turbines. Therefore, the theoretical maximum power from the SUT turbines cannot be calculated according to the Betz' law (Fluri and von Backström, 2008a; Li et al., 2012b). The use of optimal turbine pressure drop factor at 16/27 is also improper for SUTPPs.

Several constants of 2/3, 0.8, 0.82, 0.85, 0.9, and 0.97 that are higher than 16/27 have been used as the optimal turbine pressure drop factor for the SUT turbines in references. Difference among the constants can be attributed to the difficulty in maximizing the plant power output which is related to too many parameters and the optimal x turbine pressure drop factor value for the constant is determined by the parameters. In order to determine the optimal x value for an SUTPP under any condition, some researchers endeavored to put forward its expressions. From the two analytical expressions of the optimal x value for the maximum fluid power reported by Von Backström and Fluri (2006) and for the maximum plant power output reported by Nizetic and Klarin (2010) respectively, the optimal x value was found to be related to the solar radiation intensity, the collector temperature rise, the air mass flow rate, the effective absorption coefficient of solar collector, the roof heat loss coefficient, the SUT height, the collector area, the ambient temperature, and so on. Another analytical expression of the optimal x value for the maximum plant power output reported by Guo et al. (2013) is equivalent to that reported by Von Backström and Fluri (2006) when n is equal to 2. The theoretical analyses (Von Backström and Fluri, 2006; Nizetic and Klarin, 2010; Li et al., 2012b; Guo et al., 2013) and CFD simulations (Guo et al., 2013) were based on assumed steady-state flow in the plants. Certainly, the predicted optimal x values are between 2/3 for a constant pressure potential, independent of flow rate (Von Backström and Fluri, 2006; Koonsrisuk and Chitsomboon 2013a) and approximately 1.

Besides, the daily variations of the optimal x value have been studied by using the Bernardes's heat transfer scheme (Bernardes and von Backstrom, 2010) and the Pretorius's heat transfer scheme (Bernardes and von Backstrom, 2010; Bernardes and Zhou, 2013b), respectively. The variation range by using either of the two heat transfer schemes is found to be far wider than those for steady-state flow, and the lowest value is out of the range from 2/3 to approximately 1. The occurrence of low optimal x values can be attributed to insufficient heat gains of the airflow inside the collector during some time (Bernardes and Zhou, 2013b).

The large difference among the optimal x values should also be ascribed to the use of different SUTPP mathematical models. Further work about the optimal x values should be conducted under comprehensive consideration of solar radiation and more influencing parameters such as SUT pressure loss coefficients, heat transfer scheme and expression, heat storage capacity, and ambient wind velocity.

3.4. Moisture

In most previous mathematical models of SUTPP, the air is assumed to be dry lacking any moisture, and the dry adiabatic lapse rate (DALR) is applied for the temperatures of the air inside and outside the plant. An International Standard Atmosphere (ISA, with a mean lapse rate of 0.0065 K/m from the ground to a height of 11 km) assumption is sometimes applied for the air outside the plant. In reality, the air moisture has some influence on the air performance, and therefore affects the SUTPP pressure potential (Kröger and Blaine, 1999; Ninic, 2006; Zhou et al., 2009a, 2010c, 2014). The influence of the moisture cannot be neglected especially for the cases where the SUTPP is integrated with an open water source. The open water source may be, for example, an open seawater for desalination (Zhou et al., 2010c), an open wet ground for agriculture purposes (Dai et al., 2003; Pretorius, 2007; Stinnes, 2010), or an open wet crop for drying purposes (Ferreira et al., 2008; Maia et al., 2009b), in the solar collector. A solar pond also may act as an open water source of the SUTPP without solar collector (Akbarzadeh et al., 2009).

The wet air has been considered by Bernardes et al. (2003) as a mixture of two ideal gases to simulate the Manzanares prototype. The simulations based on the meteorological data were shown to accord with the measurements in the prototype. However, further analyses about the influence of moisture on the simulation results have not been discussed.

Kröger and Blaine (1999) pointed out that the air moisture inside the SUTPP could help enhance the plant pressure potential when the DALR or the ISA assumption with a constant lapse rate is applicable outside the SUTPP. However, since the air inside a conventional SUTPP generally comes from the ambient atmosphere on the ground level, moisture of air inside the collector is the same as that of the atmosphere on the ground level. In this case, the air moisture has a small negative effect on the pressure potential of sloped-collector SUTPP, which is suitable for conventional SUTPPs (Zhou et al., 2014). In other words, low moisture content is better for SUTPP operation only if the vapor condensation along with the release of latent heat does not occur.

Ninic (2006) studied the impact of humidity on the height potential of SUTPP. The latent heat released from the vapor condensation of the moistened air was shown to help increase the height potential. When the vapor condensation of the moistened air occurs in high enough SUT, the latent heat released could also increase the air temperature (Zhou et al., 2014), hence, enhance the pressure potential. However, it will require a lot of energy to moisten the air entering through the inlet from the atmosphere in the collector. More than six times in excess of the solar energy needed by dry collector would be used for producing saturated air at the same temperature rise for dry air, and this leads to large reduction of the efficiency of the collector filled with saturated air (Ninic, 2006).

Please cite this article in press as: Zhou, X., Xu, Y. Solar updraft tower power generation. Sol. Energy (2014), http://dx.doi.org/10.1016/j.solener.2014.06.029

Based on the assumption that dry air enters through the collector inlet, the power output from the SUT turbines of a 500 m high SUTPP open to seawater under the collector roof was approximately 30.4% of that of the same plant without open to seawater (Zhou et al., 2010c). This would result in revenue loss, though a part of the resulting revenue loss could be offset by the revenue from additional fresh water products. Therefore, it is preferable to admit ambient air with high moisture into the collector from the point of view of height potential and pressure potential, but it is not cost effective to use solar energy to moisten the air in the collector.

Once a commercial SUTPP is built and starts operation, a large amount of warm plume will flow from high SUT outlet into the atmosphere at high altitude continuously. This only could result in a local atmospheric circulation, if the plume is assumed to be dry. In fact, the humidity content of the plume coming from the ground is much higher than that at an elevated height. When the plume rises, its temperature drops, and its relative humidity becomes higher than the suroundings. In addition, abundant tiny granules transported in the SUT updraft coming from the ground can be used as effective condensation nuclei of vapor (Zhou et al., 2008; VanReken and Nenes, 2009). Therefore, besides the local atmospheric circulation, a cloud system would probably form around the SUTPP, which can increase the probability of rainfall in the local area. A special climate can then form around a commercial SUTPP (Zhou et al., 2008). The humidity content of the plume could determine the dimension of the cloud system. The lower-velocity ambient winds at high altitude and the latent heat released from vapor condensation also could aid the plume to rise to a higher altitude (Zhou et al., 2009a).

3.5. Ambient winds

Ambient winds will influence SUTPP performance in three main ways: by producing the convective heat loss from the collector roof to the environment, by blowing the indoor heated air through the collector and to the outside of the collector rather than up the SUT, and by generating a suction effect through the SUT outlet to increase the updraft in SUT. The first two processes will lead to a reduction of collector efficiency, while the last one will result in the increase in SUT efficiency. The convective heat loss by the first process has been included as the term q_{ra} in the energy equation (Eq. (5)) of common mathematical models for SUTPP. The quantity is determined by the heat transfer coefficients from the roof to the environment as discussed in Section 3.1.1.

The heat loss by the second process has not been included in the common mathematical models of SUTPP, but has been investigated based on logarithmic ambient wind velocity profiles using CFD simulations by Serag-Eldin (2004a, 2004b) and Ming et al. (2012, 2013b). Serag-Eldin (2004a) predicted the effect of ambient winds on the SUTPP performance by neglecting the convective heat loss from the collector roof to the environment whereas Ming et al. (2012) did similar work by considering the convective heat loss from the collector roof to the environment. It was concluded that comparably weak ambient winds would deteriorate the SUTPP performance due to the ambient winds blowing the indoor heated air through the collector and to the outside of the collector, whereas strong enough ambient crosswinds might slightly increase the air mass flow rate due to a suction effect at the SUT outlet (Ming et al., 2012).

In Pretorius (2007)'s comprehensive SUTPP model, except for the heat loss by the second process, the heat loss by the first process and possible gain by the last process due to ambient winds have been considered. Numerical simulations with this model showed that the annual power output of the proposed commercial SUTPP for a linear ambient wind velocity profile with a value of 2 m/s at 10 m height dropped by approximately 11% from that under quiet ambient conditions (Pretorius and Kröger, 2009). The power reduction mainly results from the convective heat loss from the collector roof to the environment. Besides, it was also found that ambient winds around the SUT outlet had a positive effect on the SUTPP power output because a suction effect is generated through the SUT outlet (Pretorius and Kröger, 2009). When the heat losses by the first two processes due to ambient winds were not considered, Zhou et al. (2012) observed a positive effect of ambient crosswinds through the SUT outlet on the SUT pressure potential and indoor updraft velocity. Even for an SUT without solar collector heating the air, ambient crosswinds were found to produce an SUT updraft with its velocity at the SUT inlet reaching 26% of the velocity of the crosswinds through the SUT outlet.

4. Non-conventional technologies

In Section 1.2, some main disadvantages of conventional SUTPP have been discussed. In order to overcome one or several disadvantages, many non-conventional technologies have been proposed. The representative concept and the characteristics of the selected non-conventional technologies are summarized in Table 8.

Some hybrid concepts of SUTPP combined with mountains have been proposed. The concepts include the sloped-collector SUTPP (Bilgen and Rheault, 2005), the sloped-tower SUTPP (Günther, 1931), the mountain hollow SUTPP (Zhou et al., 2009c), and the segmented floating tower SUTPP (Zhou and Yang, 2009). The hybrid SUTPPs can reach a high height with high safety when constructed next to mountains in steady-geology regions. The sloped-collector SUTPP has become a hot study area because of high thermal performance and an additional "SUT" effect of the ascending collector (Bilgen and Rheault, 2005). The investment of the sloped-collector SUTPP may be much lower than that of conventional SUTPP having the same power capacity (Cao et al., 2013b). A trapezoidal-shaped

Please cite this article in press as: Zhou, X., Xu, Y. Solar updraft tower power generation. Sol. Energy (2014), http://dx.doi.org/10.1016/j.solener.2014.06.029

Table 8
Representative concepts and characteristics of selected non-conventional technologies.

Representative concept	Category	Typical products	Advantages	References
Sloped collector	Combined with mountain	Electricity	High thermal performance, additional "SUT" effect, and high safety	Bilgen and Rheault (2005), Cao et al. (2011, 2013b, 2013c), Panse et al. (2011), Koonsrisuk (2012, 2013), Zhou et al. (2013d, 2014) and Kalash et al. (2013)
Sloped SUT	Combined with mountain	Electricity	High safety	Günther (1931)
Mountain hollow as SUT	Combined with mountain	Electricity	High safety	Zhou et al. (2009c)
Segmented floating SUT	Combined with mountain and soft SUT	Electricity	Easy and safe to reach high height	Zhou and Yang (2009)
Trapezoidal-shaped collector	Combined with landfill	Electricity	To impel harmful landfill gases to upper levels, and to reclaim closed landfill areas	Stamatov (2010)
Floating SUT	Soft SUT	Electricity	Easy to reach high height	Senanayake (1996), Papageorgiou (2003), Zhou and Yang (2009) and Zhou et al. (2009b)
Inflatable free-standing flexible SUT	Soft SUT	Electricity	Easy to reach high height, and stable structure	Putkaradze et al. (2013)
Solar pond as heat source	Instead of collector	Electricity	Easy to control power output, and no need of collector	Golder (2003) and Akbarzadeh et al. (2009)
Industrial hot water as heat source	Instead of collector	Electricity	To capture waste heat and no need of collector	Chen et al. (2014)
Greentower	Multiple products	Electricity and agricultural products	Cost-effective	Thomashausen (2010), Stinnes (2010), Hummel (2010) and Ademes (2010)
Hybrid seawater desalination	Multiple products	Electricity, fresh water, and even raw materials of crude salts	Cost-effective	Zhou et al. (2010c), Zuo et al. (2011, 2012) and Niroomand and Amidpour (2013)
Solar cyclone	Multiple products	Electricity and fresh water	Cost-effective	Kashiwa and Kashiwa (2008)
Tornado-type wind tower installed at SUT outlet	Improving performance	Electricity	To enhance ventilation effect	Li et al. (2012a)
Wind channel installed at SUT outlet	Improving performance	Electricity	To enhance ventilation effect	Zhou et al. (2013a)
Double glazed collector roof	Improving performance	Electricity	To enhance power output	Bernardes et al. (2003) and Pretorius (2007)
Solar pond(s) as additional external heat source(s)	Improving performance	Electricity	To enhance power output	Davey (2006) and Zhou et al. (2009f)
Hot exhaust gases from a nearby gas turbine power plant as additional external heat source	Improving performance	Electricity	To enhance power output and capture waste heat	Islamuddin et al. (2013)
Geothermal hot water as additional external heat source	Improving performance	Electricity	To enhance power output	Cao et al. (2014)
Collector with controllable flaps or a blockage installed around the periphery	Improving performance	Electricity	To reduce heat loss due to ambient winds blowing indoor heated air to outside of collector	Serag-Eldin (2004b) and Ming et al. (2013b)
Enclosed collector	Improving performance	Electricity	Easy to control power output	Papageorgiou (2013)
Collector with secondary roof and possible multiple radial channels under it	Improving performance	Electricity	Easy to control power output	Pretorius (2007)
Collector with a double glazed secondary roof	Improving performance	Electricity	Easy to control power output	Pretorius (2007)
Collector with a secondary and tertiary roof	Improving performance	Electricity	Easy to control power output	Pretorius (2007)

Please cite this article in press as: Zhou, X., Xu, Y. Solar updraft tower power generation. Sol. Energy (2014), http://dx.doi.org/10.1016/j.solener.2014.06.029

Table 8 (*continued*)

Representative concept	Category	Typical products	Advantages	References
Collector with auto-movable roof	For practical use	Electricity	To be automatically unloaded	Zhou et al. (2013b)
Modular collector	For practical use	Electricity	To be assembled with less works and lower cost	Papageorgiou and Katopodis (2009)
Collector with ribs and their branchings	For practical use	Electricity	To reduce the friction loss and construction cost	Bonnelle (2004)
Hybrid cooling tower	Another use and even outputting power	Cooling and even electricity	To enhance cooling rate and even to capture rejected heat	Zou et al. (2012, 2013, 2014) and Zandian and Ashjaee (2013)
Drying only	Another use	Dried agricultural products	Good drying effect and suitable for small dimension	Ferreira et al. (2008) and Maia et al. (2009b)
Seawater desalination only	Another use	Fresh water, and even raw materials of crude salts	To enhance desalination effect	Khoo et al. (2011)

collector SUTPP constructed over a landfill was proposed by Stamatov (2010) to impel large volumes of harmful landfill gases from lower to upper levels of the atmosphere.

Three concepts of soft SUTs instead of reinforced concrete SUT have been proposed. Specifically, two concepts of floating SUT with the help of buoyant-gases-filled units were invented by Senanayake (1996) and Papageorgiou (2003), respectively, and an inflatable self-supporting, free-standing flexible SUT with the help of air-filled units was proposed by Putkaradze et al. (2013). The soft SUTs can readily reach very high height with very high safety and low cost (Papageorgiou, 2003; Zhou et al., 2009b; Putkaradze et al., 2013). A solar pond (Golder, 2003; Akbarzadeh et al., 2009) and industrial hot water (Chen et al., 2014) were respectively proposed to substitute for solar collectors as heat sources of the air current moving towards the SUT.

Some novel concepts of combined SUTPP for both producing electric power and other purposes of agriculture (Thomashausen, 2010; Stinnes, 2010; Hummel, 2010; Ademes, 2010), desalination (Zhou et al., 2010c; Zuo et al., 2011, 2012; Niroomand and Amidpour, 2013), or harvesting atmospheric water (Kashiwa and Kashiwa, 2008) have been proposed. The combined systems are expected to produce both electric power and other products to improve the cost effectiveness. The concepts refer to vaporization or condensation process.

In order to enhance the plant power, some effective measures have been proposed to improve the energy conversion efficiency, to lessen the collector heat losses, or to obtain heat from additional external heat source. A tornado-type wind tower (Li et al., 2012a) and a wind channel (Zhou et al., 2013a) were respectively proposed to be installed at the SUT outlet to increase the updraft in the SUTPP. Double glazed collector roof was put forward to substantially reduce the convective heat loss from the roof (Bernardes et al., 2003; Pretorius, 2007). Controllable flaps (Serag-Eldin, 2004b) and a blockage (Ming et al., 2013b) were respectively proposed to be installed around the periphery to reduce the heat loss due to the ambient winds blowing the indoor heated air through the collector and to the outside of the collector. Solar pond(s) (Davey, 2006; Zhou et al., 2009f), hot exhaust gases from a nearby gas turbine power plant (Islamuddin et al., 2013), and geothermal hot water (Cao et al., 2014) were respectively proposed as additional external heat sources of SUTPP mainly to help it work during night time.

To control and enhance SUTPP power output profile, apart from laying closed water-filled heat storage system down on the ground (Kreetz, 1997; Schlaich et al., 2005; Bernardes and Zhou, 2013a), some modifications of the conventional collector were proposed by Pretorius (2007), which include the incorporation of an intermediate secondary roof and possible further implementation of multiple radial channels under it, the incorporation of a double glazed secondary roof, and the incorporation of a secondary and tertiary roof. In the modified collector, the collector airflow area was regulated by an airflow regulating mechanism at the collector outlet to achieve effective control of the power output. Papageorgiou (2013) proposed an enclosed solar collector encircled by a peripheral wall, in which some electro-mechanical air stop systems were used to control the number of open openings separately to adjust the SUTPP power output.

In vast regions suitable for commercial SUTPP construction sites, SUTPPs will be probably confronted by dust and sand weather (Höffer et al., 2010, 2012), or snow and ice weather (Kuck et al., 2010), and the collector may encounter overloads. In order to solve the problem of solar collector resisting the overloads, Zhou et al. (2013b) designed a novel solar collector with an auto-movable roof for unloading. The collector can be automatically unloaded without any other energy input and addition of operation costs, except for a little additional investment on the necessary components as compared to conventional solar collector. Since the construction of vast solar collector on desert is laborious and expensive, Papageorgiou and Katopodis (2009) proposed a modular solar collector constituted by parallel series of reverse V transparent tunnels. The tunnels can be assembled on site with less effort and lower cost. In

Please cite this article in press as: Zhou, X., Xu, Y. Solar updraft tower power generation. Sol. Energy (2014), http://dx.doi.org/10.1016/j.solener.2014.06.029

Fig. 4. Picture of Manzanares pilot plant prototype (Schlaich, 1995).

Fig. 5. Picture of Wuhai pilot plant (Qin, 2013).

order to reduce the friction losses effectively, a collector concept with ribs containing their branchings was proposed by Bonnelle (2004). Compared with the conventional collector, this new design has larger entrance area, which leads to smaller air velocity, thus lower friction loss. Accordingly, the roof can be lowered and then the collector construction cost reduced.

A hybrid SUT cooling tower concept was proposed to generate additional updraft force for higher cooling rate (Zou et al., 2012, 2013, 2014), and even to capture the rejected heat from the condenser into dry cooling tower to generate electricity (Zandian and Ashjaee, 2013). SUT was not proposed for producing electric power but for sole purpose of drying (Ferreira et al., 2008; Maia et al., 2009b) or desalination (Khoo et al., 2011).

5. Experiment

In the past decades, after the construction of the Manzanares pilot plant prototype, the Wuhai pilot plant and other small experimental setups were built and tested with a view of taking measurements of important parameters for use in many countries. The main structural parameters and technical data of the Manzanares plant (Fig. 4) (Schlaich et al., 2005) and the Wuhai plant (Fig. 5) (Wei and Wu, 2012) are presented in Table 9. The measured operational data, e.g., solar radiation, and power output of the Manzanares plant on a typical day and the Wuhai plant during a time span of a day are shown in Fig. 6. The measurements from the Manzanares plant have always been used to validate mathematical models by researchers. The Wuhai plant started operation in the desert region of Jinshawan in Wuhai City of Inner Mongolia Autonomous Region in North China in October 2010. Due to the restriction of the requirements of airport clearance protection, the 53 m high SUT built near the Wuhai airport is much lower than expected. This leads to only approximately 3 kW of power output under weak ambient windy conditions for average ambient wind velocity of lower than 2 m/s (Wei and Wu, 2012). Different from the Manzanares plant, some openings in the peripheral wall of the Wuhai plant were used to control the mass flow rate of the ambient winds entering the collector by opening and closing them. The measurements showed the ambient winds have a significant effect on the mass flow rate of air inside this

Table 9
Main structural parameters and technical data of Manzanares plant (Schlaich et al., 2005) and Wuhai plant (Wei and Wu, 2012).

Item	Schlaich et al. (2005)	Wei and Wu (2012)
Location	39°02′34.45″N 3°15′12.21″W	39°46′03.25″N 106°49′49.25″E
SUT height (m)	194.6	53
SUT radius (m)	5.08	9.25
Collector shape	Approximate circular shape	Ellipse shape
Collector radius or area	122 m (radius)	6170 m^2 (area)
Turbine configurations and layouts	Vertical-axis single-rotor type	Horizontal-axis single-rotor type
Number of turbine blades	4	3
Operation modes	Stand-alone or grid connected mode	Stand-alone or grid connected mode
Collector air temperature rise (K)	20 (Typical value)	–
Nominal power output (kW)	Approximately 50 (Peak)	Approximately 3[a]
Collector covered with plastic membrane (m^2)	40,000	0
Collector covered with glass (m^2)	6000	6170

[a] The measured power output for average ambient wind velocity of lower than 2 m/s.

Please cite this article in press as: Zhou, X., Xu, Y. Solar updraft tower power generation. Sol. Energy (2014), http://dx.doi.org/10.1016/j.solener.2014.06.029

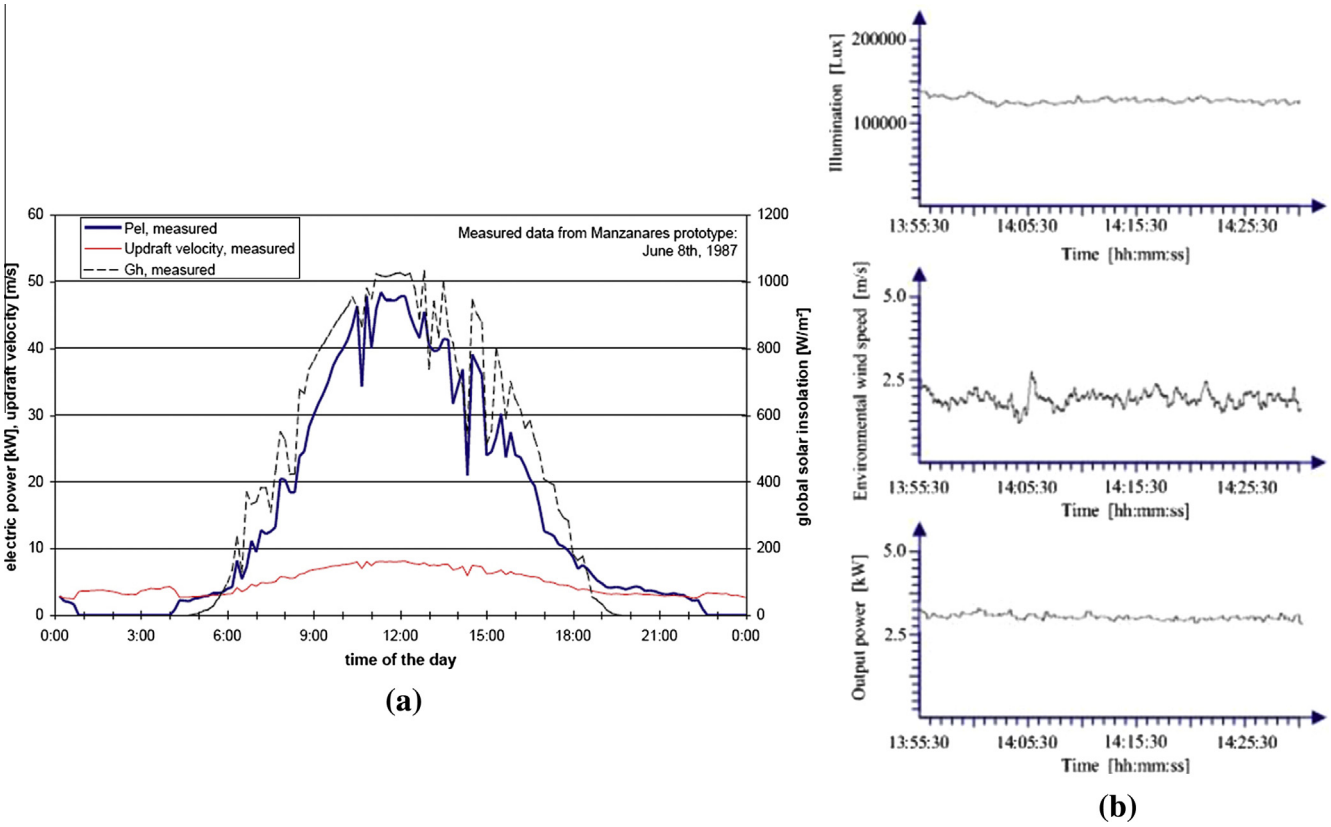

Fig. 6. Measured power outputs of (a) Manzanares plant on June 8, 1987 (Schlaich et al., 2005) and (b) Wuhai plant from 13:55:30 to 14:25:30 p.m. on December 29, 2010 (Wei and Wu, 2012).

plant with a small collector the area of which is 13.4% of that of the Manzanares plant.

The main structural parameters and technical data of small experimental SUTPP setups built in many countries are presented in Table 10. The largest collector among these setups is 1020 m^2 in area, and the highest SUT among them is 60 m in height. Generally, the main work related to the setups was to study the SUT system performance by mainly testing the temperature and velocity of the air current. In some locations, the effects of dimensions, SUT shape, collector design parameters, cover materials, ground heat storage materials and so on, on the performance of SUT setups were also studied. Except for several non-conventional SUT setups, the setups were the prototypes of the conventional SUTPP, where similar temperature distributions and low velocities were obtained. The ambient winds always have a significant influence on the air parameters especially the mass flow rate in far smaller collectors than the collector of the Wuhai plant (Motsamai et al., 2013). However, little work on analyzing the respective contribution of buoyancy due to solar radiation and ambient winds on the air mass flow rate inside the collector has been reported. The experimental work about the basic SUTPP performance has laid down a solid foundation for development of mathematical models on which commercial SUTPPs can be predicted and carefully designed.

6. Power production conditions

It is important to note that suitable conditions for obtaining high performance of SUTPP should be taken into account. In order to produce electric power from SUTPP, four good conditions should be satisfied, that is, large enough size, good climate conditions, cheap local construction materials and labor force, and vast desert region. Correlations of commercial SUTPP power output and main factors are demonstrated in Table 11.

All of the SUT height, collector diameter, solar radiation, local construction material prices, labor force cost, and land value are the important factors to determine the cost-effectiveness of power output from SUTPP. Firstly, the SUT power generation has strong effects of scale economies, implying that the energy cost decreases with its size. A larger collector area leads to a higher collector air temperature, while a higher SUT produces a stronger updraft in it. A larger-scale SUTPP can induce a higher power output and a lower LEC. Secondly, as a typical solar radiation dependent device, SUTPP needs abundant solar radiation. The SUTPP should generally be constructed in the regions with average annual global solar radiation on a horizontal surface exceeding 1950 kW h/(m^2 a). The level of higher than 2200 kW h/(m^2 a) will be better, as stated in Schlaich (1995). Thirdly, low prices of local construction

Please cite this article in press as: Zhou, X., Xu, Y. Solar updraft tower power generation. Sol. Energy (2014), http://dx.doi.org/10.1016/j.solener.2014.06.029

Table 10
Main structural parameters and technical data of small experimental SUTPP setups.

No	Site	SUT height (m)	SUT diameter (m)	Collector diameter/ area	Roof material	Velocity in SUT[a] (m/s)	Collector temperature rise[a] (K)	Construction date (year)	References
–	Connecticut, USA	10	–	6 m	–	–	–	1983	Krisst (1983)
–	Izmir, Turkey	2	0.07	9 m^2	–	–	–	1985	Kulunk (1985)
(a)	Florida, USA	7.92	2.44–0.61[b]	9.14 m	Plastic	–	13.9[d]	1997	Pasumarthi and Sherif (1998b)
	Florida, USA	7.92	2.44–0.61[b]	18.3 m	Plastic	–	27.8[d]	1997	Pasumarthi and Sherif (1998b)
	Florida, USA	7.92	2.44–0.61[b]	18.3 m	Plastic	3.1[c]	28.1[d]	1997	Pasumarthi and Sherif (1998b)
(b)	Bundoora, Australia[e]	8	0.35	4.2 m	–	1	11	2002	Golder (2003) and Akbarzadeh et al. (2009)
(c)	Wuhan, China	8.8	0.3	10 m	Glass	2.81	24.1	2002	Zhou et al. (2007a)
(d)	Belo Horizonte, Brazil[f]	12.3	1	25 m	Plastic	2.9[c]	27 ± 2	2003[g]	Ferreira et al. (2006) and Maia et al. (2009b)
(e)	Isparta, Turkey	15	1.2	16 m	Glass	–	–	2004	Koyun (2006) and Üçgül and Koyun (2010)
(f)	Kerman, Iran	60	3	40×40 m^2	Glass	–	–	2005[h]	Najmi et al. (2012) and Koyun (2006)
(g)	Berlin, Germany	–	–	–	–	–	–	2006[h]	Koyun (2006)
(h)	Gaborone, Bostwana	22	2	15×15 m^2	Glass	7.5[c,i]	6.8[c]	2008[g]	Motsamai et al. (2013)
(i)	Weimar, Germany	12	–	420 m^2	Plastic	2.42[d]	17.2[d]	2008	Hartung et al. (2008)
(j)	Nanjing, China[j]	2.5	0.08	–	Glass	–	14	2008[g]	Zuo et al. (2012)
(k)	Baghdad, Iraq	4	0.2	6 m	Plastic	2.309	22	2009[g]	Ahmed and Chaichan (2011)
(l)	Karak, Jordan	4	0.58	36 m^2	Plastic	–	–	2009	Al-Dabbas (2011a)
(m)	Gafsa, Tunisia	16	0.4	15 m	Glass + Plastic[k]	–	–	2009	Dhahri and Omri (2013)
(n)	Nakhon Ratchasima, Thailand	8	2	8[l] m	Plastic	–	–	2009	Koonsrisuk (2009)
(o)	Nakhon Ratchasima, Thailand	8	2 to 2.82[m]	8[l] m	Plastic	–	–	2009	Koonsrisuk (2009)
(p)	Nakhon Ratchasima, Thailand	8	2	8.2[n] m	Plastic	–	–	2009	Koonsrisuk (2009)
(q)	Nakhon Ratchasima, Thailand	4	1	3.36[l] m	Plastic	–	–	2009	Koonsrisuk (2009)
(r)	Zanjan, Iran	12	0.25	10 m	Plastic	2.9	26	2010	Kasaeian et al. (2011)
(s)	Kompotades, Greece[o]	–	–	–	–	–	–	2010	Papageorgiou (2013)
(t)	Adıyaman, Turkey	17.15	0.8	27 m	Glass	5.5[c]	26	2010	Buğutekin (2012)
(u)	Pau, France	2.5	0.041	3.65 m^2	Plastic	–	–	2011[p]	Manon et al. (2011)
(v)	AlAin, United Arab Emirates	8.25	0.24	10×10 m^2	Plastic	3.4[c]	26.8[c]	2011[g]	Mohammad and Obada (2012)
(w)	Hamirpur, India	0.8	(I) 0.08, (II) 0.10, (III) 0.12	1.4 m	Plastic	(I) 0.49[c], (II) 0.45[c], (III) 0.36[c]	(I) 1.7[c], (II) 2.5[c], (III) 3.2[c]	2011	Mehla et al. (2011)

Table 10 (*continued*)

No	Site	SUT height (m)	SUT diameter (m)	Collector diameter/ area	Roof material	Velocity in SUT[a] (m/s)	Collector temperature rise[a] (K)	Construction date (year)	References
(x)	Karnataka, India	4	0.24	3	–	1.2	–	2011	Bekal (2013)
(y)	Texas, USA[q]	5.08	0.19	11.58	Plastic	2[e]	–	2012[p]	Raney et al. (2012)
(z)	Damascus, Syria[r]	9	0.31	12.5 m^2	Glass	2.9	19	2012[g]	Kalash et al. (2013)
(aa)	New Jersey, USA	7.1	–	100 m^2	Plastic	–	–	2012	Herrick (2013)
(ab)	Kompotades, Greece[s]	25	2.5	1020 m^2	Plastic	–	–	2013	Papageorgiou (2013)
(ac)	Tehran, Iran	2	0.2	3 m	Glass	1.3	11.05	2013	Kasaeian et al. (2014)

[a] The data are the maximum values measured and listed in the references. The velocity and the collector temperature rise may not match each other.
[b] The SUT was convergent.
[c] The values are obtained from the figures in the references.
[d] The values are obtained from the tables in the references.
[e] Solar pond instead of collector was used as heat source.
[f] Used as drier for sole drying.
[g] The construction dates were not mentioned in the references. The years when the experiments were conducted are given.
[h] The construction dates were not mentioned in the references. The years when Koyun (2006) visited the websites about the setups are given.
[i] The maximum SUT velocity of about 7.5 m/s and the corresponding collector temperature rise of about 6.23 K were measured at the ambient wind velocity of about 2.5 m/s at 12:37 of a day, while the minimum SUT velocity of about 2.5 m/s and the corresponding collector temperature rise of about 2.11 K were measured at the ambient wind velocity of about 1.1 m/s at 20:37 of the day.
[j] Hybrid system for both power production and seawater desalination.
[k] The inner and outer covers of the collector were glass and plastic, respectively. The distance between the two covers was less than 2.5 cm.
[l] The collector was octagonal, and the length of its diagonal line is given.
[m] The SUT was divergent.
[n] The collector was approximately squared with four openings at the four corners, and the length of its symmetric line through the geometric centers of two openings is given.
[o] Floating SUT.
[p] The construction dates were not mentioned in the reference, and the publication years of the references are given.
[q] The experiments were conducted by varying SUT height, SUT diameter, collector roof slope and roof material.
[r] Sloped-collector SUTPP.
[s] Enclosed-collector SUTPP.

materials and low cost of labor force are necessary for SUTPPs with enough low LECs. Finally, a great amount of lands are needed for large-scale SUTPP. In order to improve the competitiveness, valuable agricultural lands should not be used as SUTPP construction sites, and only low- or no-valuable lands like desert lands are suitable for SUTPP sites.

The global distribution of average annual global solar radiation on a horizontal surface based on daily data averaged from July 1983 to June 2005 is shown in Fig. 7. The global distribution of the desert lands based on the data in 2011 is shown in Fig. 8. As shown in the two figures, most of the barren or sparsely vegetated lands and open shrub lands, mainly including the Sahara Desert, the Arabian Peninsula Deserts, the Australian Desert, the Kalahari Desert, the Atacama Desert, the deserts in Iran and the surrounding regions, the North American Desert, the Taklimakan Desert, and the Gobi, where solar radiation is abundant, are suitable for SUTPP sites. The potential power production from SUTPPs is considerable. This can be achieved by making full use of abundant solar radiation on desert lands.

7. Energy cost estimate

The economic competitiveness of the SUTPPs is one of main factors to influence the development and commercialization of the technology, which was always evaluated by using the estimated LECs. The LEC is defined as the static electricity cost per unit electricity output during the service life of the SUTPP, which is calculated by dividing the total cost by the total electricity output or by dividing the equivalent annual cost by the annual electricity output during the service life (Schlaich, 1995; Fluri et al., 2009; Zhou and Yang, 2009). It can be expressed as

$$\mathrm{LEC} = \frac{\left(\frac{C_{om}}{inf-i}\left(\left(\frac{1+inf}{1+i}\right)^N - 1\right) + C_{ii}\right)\left(\frac{i(1+i)^N}{(1+i)^N-1}\right)}{P} \tag{32}$$

where C_{om} is the operation and maintenance (O & M) cost in the first year of the service life, C_{ii} is the capital cost, inf is the inflation rate, i is the interest rate, N is the length of the service life and P is the annual electricity output.

The details of the annual electricity outputs, the initial investment costs, the O & M costs, and the LECs of the

Table 11
Correlations of commercial SUTPP power output and main factors.

Factors	Correlation	References
Solar radiation	PC	Schlaich (1995)
Atmospheric temperature	NC	Schlaich (1995) and Zhou et al. (2010a, 2014)
Diurnal temperature range	PC	Zhou and Yang (2009)
Moisture content	NC	Zhou et al. (2014)
Wind velocity [a]	NC	Pretorius (2007) and Pretorius and Kröger (2009)
Static pressure	PC	Zhou et al. (2014)
SUT height	PC	Schlaich (1995)
Collector diameter	PC	Schlaich (1995)
Land value	NC	Schlaich (1995) and Li et al. (2014)
Local labor force cost	NC	Li et al. (2014)
Local transportation price	NC	Li et al. (2014)
Local construction material price	NC	Li et al. (2014)
Grid connection costs	NC	–
Electricity transmission losses	NC	–

PC: Positive correlation and NC: Negative correlation.

[a] The heat loss due to ambient winds blowing the indoor heated air through the collector and to the outside of the collector is assumed to be eliminated by taking some effective measures, for example, installing controllable flaps (Serag-Eldin, 2004b) or a blockage (Ming et al., 2013b) around the periphery. In this case, ambient winds will influence SUTPP performance in two main ways: by producing the convective heat loss from the collector roof to the environment, and by generating a suction effect through the SUT outlet to increase the updraft in SUT.

commercial SUTPPs in literature are summarized in Table 12. The estimated LECs of the plants change in a wide range. However, only three plant LECs are higher than 0.15 €/kW h. The LECs of the 8.2 MW plant estimated with various parameters ranged from 0.24 to 0.78 €/kW h (Nizetic et al., 2008), which are attributed to far smaller dimensions than the other plants with the power capacities of higher than or equal to 28.8 MW. The LECs of the two 100 MW plants estimated by Fluri et al. (2009) are much higher, which is mainly due to much higher initial investment costs and lower electricity outputs than those by Schlaich et al. (2004), Bernardes (2004), Cao et al. (2013b) and Li et al. (2014). Higher initial investment costs by Fluri et al. (2009) are mainly induced by higher collector costs. This is mainly because compared to the tempered glass covered collectors used by Fluri et al. (2009), all of the materials for the glass covered collector used by Schlaich et al. (2004), for the glass covered collector used by Bernardes (2004) and for the (tempered) glass covered collector in China (Cao et al., 2013b; Li et al., 2014) are much cheaper. Lower electricity outputs by Fluri et al. (2009) are attributed to the use of Pretorius (2007)'s comprehensive SUTPP model that are different from the other research groups' models.

The amortization period used for estimating LEC in literature is always between 15 and 40 years. In fact, intended designed service lives of commercial SUTPPs are 80–120 years (Von Backström et al., 2008; Krätzig et al., 2009; Harte et al., 2013) and even more than 120 years (Krätzig, 2013), admitting renewals of the turbo-generators and parts of the glass-roof. Taking the 100 MW SUTPP designed by Schlaich et al. (2004) as an example, the variation of LEC estimated using Eq. (32) based on Fluri et al. (2009)'s economic parameters and estimated electricity output with amortization period is shown in Fig. 9. With an increase in amortization period, LEC intially decreases negative exponentially but remains little changed when the amortization period exceeds 40 years. In order to indicate the benefits induced by long service life, the SUTPP service life was divided into several service phases (Zhou et al., 2009b, 2009c; Li et al., 2014). The loans are amortized in the first phase, and the SUTPP is considered to be free for further use for producing power except for a little O & M cost in other phases.

It is concluded that larger-scale SUTPPs located in the regions where solar radiation is abundant and the main construction materials are cheap are competitive with other renewable energy power technologies and even with coal-fired power plants with rising coal price in the future. Once the benefits due to long service lives are considered, larger-scale SUTPPs are more competitive and even some profits could be produced. Additional revenue generated by carbon credits could result in a reduced LEC. The financial incentives and strategies such as a non-returnable subsidy, enhanced feed-in tariffs, soft loans with low interest rates, and favorable income tax waivers could further improve the competitiveness of SUTPPs.

8. Environmental impacts

Besides abating the emissions of greenhouse gases, and avoiding the use of potable water for cooling purposes, SUTPP operation can help in soil rehabilitation, forestry, and desert cultivation at local regions (Stinnes, 2010). The SUTPP can be used to suppress air pollutions in cities by spraying water at the SUT outlet to force the airflow downward (Lodhi, 1999). The technology was also proposed to impel large volumes of harmful landfill gases from lower to upper levels of the atmosphere to reduce the environmental impacts of uncontrolled emissions of the harmful landfill gases to the neighboring areas (Stamatov, 2010). The special climate induced by the continuous air outflow from a high SUT as described in Section 3.4 can have a positive effect on the local environment and atmosphere, and produce some positive ecological effects (Zhou et al., 2008, 2009a).

However, similar to other renewable energy utilizing technologies, some negative environmental impacts exist for large-scale application of SUTPP technology. Environmental concerns have come up in the use of solar panel arrays in some parts of the US Southwest (Wikipedia, 2014). The SUTPP project would face significant challenges due to the collector expanse. Super-high SUTs may affect the normal movement of aircrafts (Wesoff, 2011). The SUTPP may affect and even endanger some plants and animals. For example, the desert tortoise

Please cite this article in press as: Zhou, X., Xu, Y. Solar updraft tower power generation. Sol. Energy (2014), http://dx.doi.org/10.1016/j.solener.2014.06.029

Table 12

Summary of estimated LECs of commercial SUTPPs.

Estimated LEC (€/kW h)	SUTPP type	Location, solar radiation (kW h/m^2 a)	Dimension					Cost							Economic parameters			References
			Power capacity (MW)	SUT height (m)	SUT diameter (m)	Collector diameter/ area	Annual electricity output (GWh/a)	SUT cost[a] (M€)	SUT price[b] (€/m^2)	Collector cost[c] (M€)	Collector price[b] (€/m^2)	PCU cost[d] (M€)	Total initial investment cost (M€)	O & M cost[e] (M€)	Amortization period (years)	Interest rate (%)	Inflation rate (%)	
0.145[f]	Convectional	–, 2400.24	100[g](36[h])	1000	176	4364 m	280	97[f]	175.43	269[f]	17.98	55[f]	421[f]	10.525[f,i]	20	10	5	Haaf et al. (1983) and Pasumarthi and Sherif (1998b)
0.1045[f]	Convectional	–, 2300	100	950	115	3600 m	305.2	68.2[f]	198.71	134.8[f]	13.24	79.8+17.2[f,j]	300.0[f]	1.0[f,k]	20	8[l]	3.5	Schlaich (1995)
0.05-0.064[f]	Convectional	–	100[h]	1000	–	2 km^2	876	–	–	–	–	–	–	–	20	–	–	Lodhi (1999)
0.1000	Convectional	–, 2300	100	1000	110	4300 m	320	156	452.00	131.0	9.02	75.0+40[j]	402.0	1.9[j]	30	6	–	Schlaich et al. (2004)
0.0370	Convectional	Petrolina, Brazil, 1946	100	850	110	4950 m	281	64.4	219.24	190.0	9.87	76.7+21.29 [j]	352.4	1.0[k]	30	8	2.5	Bernardes (2004)
0.24–0.78	Convectional	Dubrovnik, Croatia, 1606	8.2[g]	550	82	1250 m	5–6	35	247.03	10	8.15	8+7.0[j]	60	3.3[i]	20-40	6-10	6	Nizetic et al. (2008)
0.270 (0.232[m])	Convectional	Sishen, South Africa, 2785.38[n]	66[g]	1000	110	4300 m	190.4	145	419.59	497	34.22	27	668.4	1.9[k]	30	6	3.5	Fluri et al. (2009)
0.434	Convectional	Sishen, South Africa, 2785.38[n]	62[g]	850	110	4950 m	181.32	111	377.89	656	34.09	25	792	1.0[k]	30	8	3.25	Fluri et al. (2009)
0.1269[o](0.1001[m,o])	Floating SUT	Northwest, China, 1800	100	–	–	4300 m	250.4[p]	89.01[f]	–[q]	232.73[f]	16.03	45.96[f]	367.71[f]	2.4[k]	15[r]	2	4	Zhou et al. (2009b)
0.1[f,s]	Mountain hollow SUT	–, 2300	100[g]	1000/ 1124[t]	124.9	19.3 km^2	210[p]	438.57[f]	994.4	81[f]	4.20	34.93[f]	554.5[f]	–	30[u]	6	3.5	Zhou et al. (2009c)
0.110[f,m]	Convectional	Lanzhou, China, 1394.44	104.7	1000	110	4300 m	–	96.64[f]	279.65	222.79[f]	15.34	50.63[f]	370.06[f]	1.9893[k]	30	6	4	Cao et al. (2013b)
0.079[f,m]	Sloped collector	Lanzhou, China, 1394.44	104.7	580	78	8.55 km^2	–	54.37[f]	382.55	156.14[f]	18.26	50.63[f]	261.15[f]	1.9893[k]	30	6	4	Cao et al. (2013b)
0.099	Convectional	–, 2200	75[g]	750	67.5, 75[v]	3500 m	219.4	60.5	360.38	213.3	22.17	48.8+15[j]	337.6	–	33[w]	–	–	Krätzig (2013)
0.1397[o](0.1294[m,o])	Convectional	–	100	1000	110	4300 m	255.2	108.03[f]	312.61	273.98[f]	18.87	69.88[f]	451.89[f]	1.9[k]	30[x]	3[y] (6)	3[y] (3.5)	Li et al. (2014)
0.1422 (0.138[m])	Conxectional	Kyrenia, North Cyprus, 1668.605[n]	28.8[g]	750	70	2900 m	94.5	49	297.09	48	7.27	32+16[j]	145	0.6[i]	20	6[y] (6)	–[y] (3.5)	Okoye and Atikol (2014)

[a] The SUT cost mainly includes the cost of materials, the transportation cost, the construction cost and the hoisting cost.

[b] The SUT price is calculated by dividing the SUT cost by the superficial area of the SUT assumed in cylindrical shape, and the collector price is calculated by dividing the collector cost by the collector area.

[c] The collector cost mainly includes the cost of materials, the transportation cost and the construction cost.

[d] The PCU cost includes the cost of the turbines, the generators, the power electronics, the ducting, the central structure, the control and the supports, the balance-of-station cost (including the cost for foundations, transportation, roads and civil works, assembly and installation, electrical interfaces and connections, permits, and engineering), the soft cost (e.g., the insurance cost), etc.

[e] The O & M cost includes the cost of cleaning the collector, maintaining the turbines, paying for staffs, etc.

[f] The exchange rates between Euro, Deutsche Mark, US dollar and Yuan (China) are: 1 Euro = 2 Deutsche Marks = 1.4 US dollars = 8.5 Yuan (China).

[g] The values were the peak power outputs.

[h] The values were the mean daily output averaged over 24 h.

[i] The values were the annual O & M costs.

[j] The values following the plus signs were the additional costs including the cost of roads, buildings and workshops, the infrastructure cost, the planning and site management cost , the rounding cost, the cost of engineering, tests, misc., the cost of electrical installations, the cost of insurance, etc., which are included in the PCU cost in this paper.

[k] The values were the O & M costs in the first year of the service life. The O & M cost increases with inflation.

[l] The value of 8% used by Schlaich (1995) was a nominal interest rate, while the other values in the table were real interest rates. The real interest rate equals the nominal interest rate subtracting the inflation rate approximately.

[m] The LEC values are estimated with the total cost subtracting the additional revenue generated by carbon credits, which are the product of the carbon credits price and the reduced CO_2 emissions due to the SUTPP operation.

[n] The annual global solar radiation values were not given in the two references. The value for Fluri et al. (2009) is estimated by authors using the data of solar radiation from Pretorius and Kröger (2006b). The value for Okoye and Atikol (2014) is estimated by authors using the data of solar radiation from Okoye and Atikol (2014).

[o] The LEC values in the first amortization phase that were not presented are calculated with Eq. (32) by authors.

[p] The annual electricity output was calculated based on the proportion of the annual global solar radiation used by Zhou et al. (2009b) to that used by Schlaich et al. (2004), or based on the simulation model established by Zhou et al. (2009c).

[q] The SUT price used by Zhou et al. (2009b) was the average of the prices of the four kinds of floating SUTs with different materials and construction shapes (Papageorgiou, 2004).

[r] The service lives of the collector and the PCU were estimated at 90 years, while the floating SUT were estimated at 15 years.

[s] The LEC value was the average of the LECs at all phases of the service life estimated using the stepwise method.

[t] The mountain was 1000 m in height, whereas the total length of the SUT hollow consisting of a sloped segment and a vertical segment was 1124 m.

[u] The life span of a mountain hollow SUT in geologically stable region could reach up to 300 years. The assumed service life of 150 years was divided into five phases at intervals of 30 years while the service lives of the collector and the turbine generators were estimated at 30 years.

[v] The throat diameter and the top diameter of SUT were 67.5 m and 75 m, respectively.

[w] The whole service life could exceed 120 years, and the plant LEC would decrease to less than 0.02 €/kW h after the first amortization period of 33 years.

[x] The assumed service life of 120 years was divided into four phases at internals of 30 years.

[y] The values were given in the two references, while the values in the brackets are used for estimating LECs by authors.

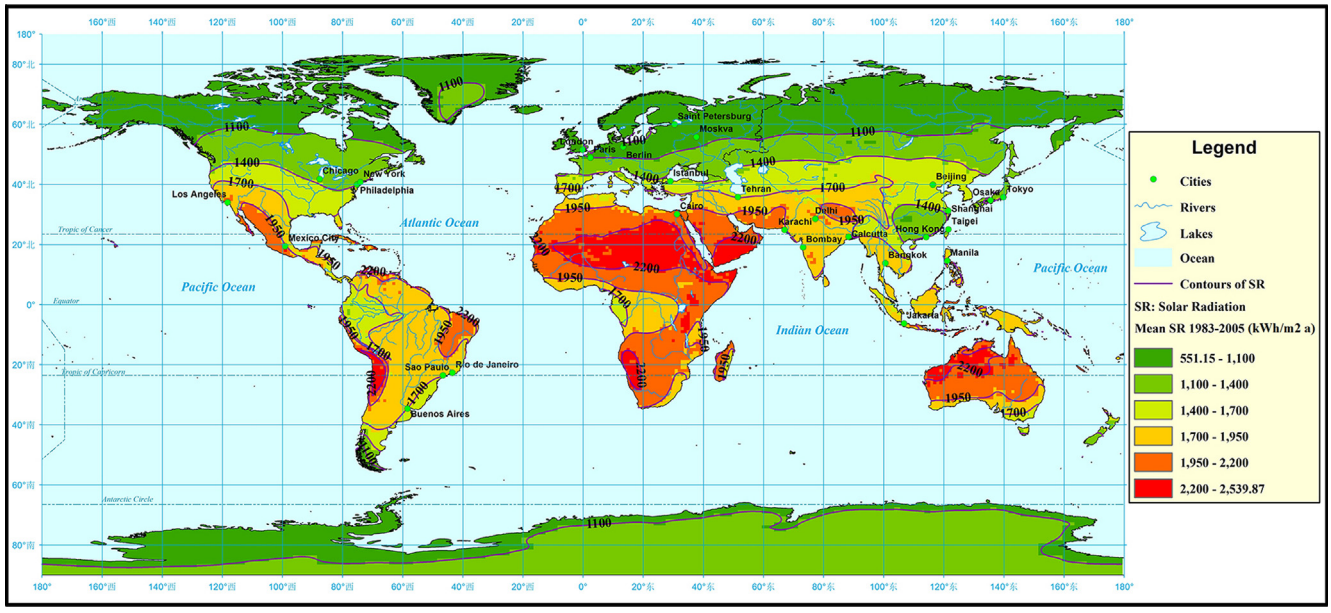

Fig. 7. Global distribution of average annual global solar radiation on a horizontal surface based on daily data averaged from July 1983 to June 2005 (NASA SSE, 2014).

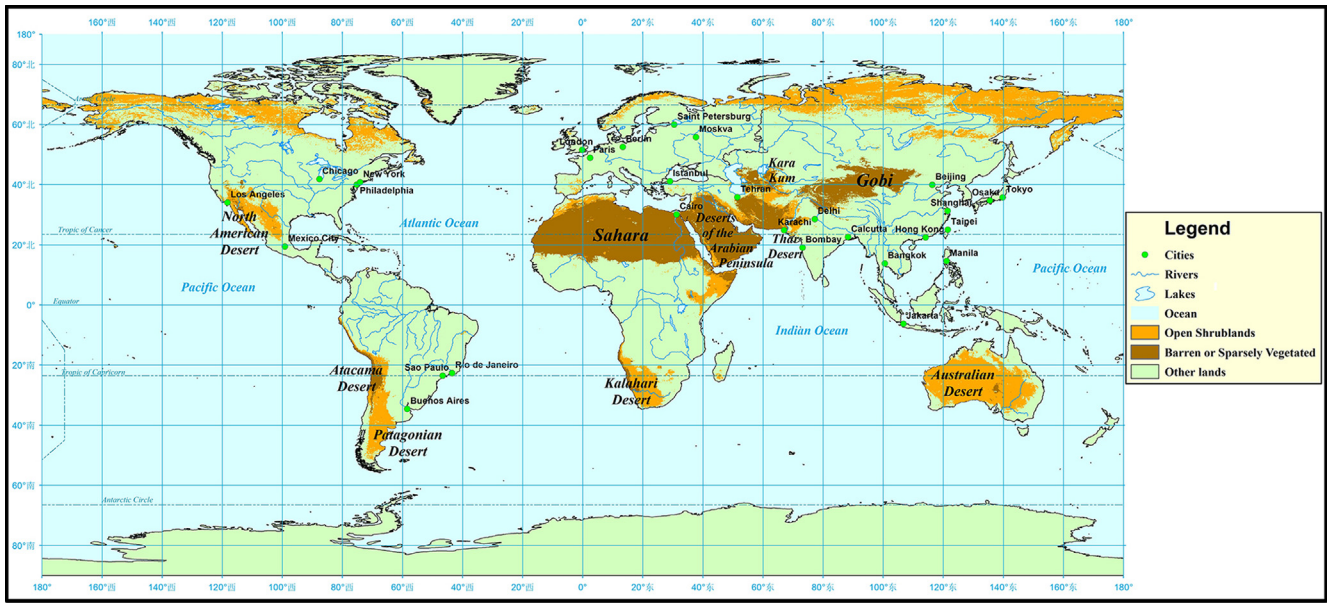

Fig. 8. Global distribution of desert lands based on the data in 2011 (NASA Earth Observations, 2014).

(*Gopherus agassizii*), an endangered species in California (Cruger, 2011), may suffer from negative effect and become extinct as the SUTPP expands there. Before commercial application of the SUTPP technology, like other new technologies, comprehensive studies of its environmental effects should be carried out.

9. Outlook and conclusions

Solar updraft towers can be used for power generation, whose technical feasibility has already been demonstrated. The technology is simple and reliable, can operate day and night, does not need any additional fossil fuels and cooling water, and is nearly pollution free during operation. Many novel non-conventional SUTPP technologies proposed can overcome one or several drawbacks and provide more choices of producing electric power under various situations. Main important factors are crucial in theoretical studies to predict the commercial SUTPP performance. Consideration of the factors in a proper manner will improve the reliability of prediction using mathematical models, which will pave the way for commercialization of the technology. Vast desert regions with strong solar radiation worldwide are suitable for SUTPP sites, implying

Please cite this article in press as: Zhou, X., Xu, Y. Solar updraft tower power generation. Sol. Energy (2014), http://dx.doi.org/10.1016/j.solener.2014.06.029

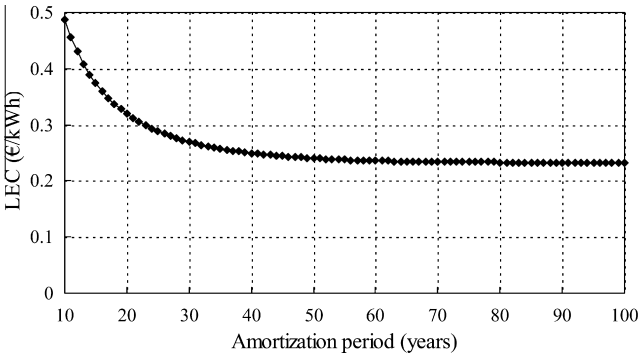

Fig. 9. Variation of LEC with amortization period of 1000 m high SUTPP of Fluri et al. (2009).

that there is a huge potential of power production from SUTPPs. The environmental impacts of concern that would be produced by the SUTPP technology should be studied properly before its commercial application. With the dwindling reserves of fossil fuels and the exacerbation of air pollution and greenhouse effect, SUTPP technology should be on the way to commercialization.

Acknowledgements

This research has been partially supported by the National Natural Science Foundation of China (No. 50908094), and the Ph.D. Programs Foundation of Ministry of Education of China (No. 20100142120071).

References

Ademes, W., 2010. Greentower with energy storage – optimum base and peak load power station. In: Proceedings of the 2nd International Conference on Solar Chimney Power Technology. Bochum, Germany, pp. 361–366.

Ahmed, S.T., Chaichan, M.T., 2011. A study of free convection in a solar chimney model. Eng. Technol. J. 29, 2986–2997.

Akbarzadeh, A., Johnson, P., Singh, R., 2009. Examining potential benefits of combining a chimney with a salinity gradient solar pond for production of power in salt affected areas. Sol. Energy 83, 1345–1359.

Al-Dabbas, M.A., 2011a. The first pilot demonstration: solar updraft tower power plant in Jordan. Int. J. Sustain. Energ. 31, 399–410.

Al-Dabbas, M.A., 2011b. A performance analysis of solar chimney thermal power systems. Therm. Sci. 15, 619–642.

ANSYS, 2012a. ANSYS CFX, Release 14.5 – Solver Theory Guide. ANSYS Inc., Canonsburg, Pennsylvania.

ANSYS, 2012b. ANSYS FLUENT, Release 14.5 User's Guide. ANSYS Inc., Canonsburg, Pennsylvania.

Asnaghi, A., Ladjevardi, S.M., 2012. Solar chimney power plant performance in Iran. Renew. Sustain. Energy Rev. 16, 3383–3390.

Asnaghi, A., Ladjevardi, S.M., Kashani, A.H., Izadkhast, P.S., 2013. Solar chimney power plant performance analysis in the central regions of Iran. J. Solar Energ. Eng. – Trans. ASME 135, 011010.

Bekal, S., 2013. Personal communication.

Bennett, A.R., 1896. Convection mill. British Patent, no. 8,711.

Bernardes, M.A.d.S., 2003. Symmetric sink flow and heat transfer between two parallel disks. In: Proceedings of the 2003 ASME Summer Heat Transfer Conference. Las Vegas, Nevada.

Bernardes, M.A.d.S., 2004. Technische, ökonomische und ökologische Analyse von Aufwind-kraftwerken. Institut für Energiewirtschaft und Rationelle Energieanwendung, Universität Stuttgart, Germany.

Bernardes, M.A.d.S., 2011. Convective heat transfer coefficients for solar chimney power plant collectors. In: Belmiloudi, A. (Ed.), Heat Transfer – Mathematical Modelling, Numerical Methods and Information Technology. Intech, Rijeka, Croati, pp. 607–620.

Bernardes, M.A.d.S., 2013. On the heat storage in solar updraft tower collectors – influence of soil thermal properties. Sol. Energy 98, 49–57.

Bernardes, M.A.d.S., von Backstrom, T.W., 2010. Evaluation of operational control strategies applicable to solar chimney power plants. Sol. Energy 84, 277–288.

Bernardes, M.A.d.S., Zhou, X.P., 2013a. On the heat storage in solar updraft tower collectors – water bags. Sol. Energy 91, 22–31.

Bernardes, M.A.d.S., Zhou, X.P., 2013b. Strategies for solar updraft tower power plants control subject to adverse solar radiance conditions. Sol. Energy 98, 34–41.

Bernardes, M.A.d.S., Valle, R.M., Cortez, M.F., 1999. Numerical analysis of natural laminar convection in a radial solar heater. Int. J. Therm. Sci. 38, 42–50.

Bernardes, M.A.d.S., Voss, A., Weinrebe, G., 2003. Thermal and technical analyses of solar chimneys. Sol. Energy 75, 511–524.

Bernardes, M.A.d.S., von Backström, T.W., Kröger, D.G., 2009. Analysis of some available heat transfer coefficients applicable to solar chimney power plant collectors. Sol. Energy 83, 264–275.

Bilgen, E., Rheault, J., 2005. Solar chimney power plants for high latitudes. Sol. Energy 79, 449–458.

Bonnelle, D., 2004. Solar Chimney, Water Spraying Energy Tower, and Linked Renewable Energy Conversion Devices: Presentation, Criticism and Proposals. Ph.D. thesis, University Claude Bernard–Lyon 1, Lyon, France.

Borri, C., Lupi, F., Marino, E., 2010. Optimum shell design of solar updraft towers. In: Proceedings of the 2nd International Conference on Solar Chimney Power Technology. Bochum, Germany, pp. 155–162.

Buğutekin, A., 2012. Experimental study of temperature field in a solar chimney plant in Adiyaman. Isi Bilimi ve Teknigi Derğisi. J. Therm. Sci. Technol. 32, 73–80.

Burger, M., 2005. Prediction of the Temperature Distribution in Asphalt Pavement Samples. M.Sc.Eng. thesis, University of Stellenbosch, Stellenbosch, South Africa.

Cabanyes, I., 1903. Las chimeneas solares (Solar chimneys). La ernergia eléctrica.

Cao, F., Zhao, L., Guo, L.J., 2011. Simulation of a sloped solar chimney power plant in Lanzhou. Energy Convers. Manage. 52, 2360–2366.

Cao, F., Li, H.S., Zhao, L., Bao, T.Y., Guo, L.J., 2013a. Design and simulation of the solar chimney power plants with TRNSYS. Sol. Energy 98, 23–33.

Cao, F., Li, H.S., Zhao, L., Guo, L.J., 2013b. Economic analysis of solar chimney power plants in Northwest China. J. Renew. Sustain. Energy 5, 021406.

Cao, F., Zhao, L., Li, H.S., Guo, L.J., 2013c. Performance analysis of conventional and sloped solar chimney power plants in China. Appl. Therm. Eng. 50, 582–592.

Cao, F., Li, H.S., Ma, Q.M., Zhao, L., 2014. Design and simulation of a geothermal–solar combined chimney power plant. Energy Convers. Manage. 84, 186–195.

Cervone, A., Romito, D.Z., Santini, E., 2011. Design of solar chimney power plant for Mediterranean countries. In: 2011 International Conference on Clean Electrical Power. Ischia, Italy, pp. 480–484.

Chen, K., Wang, J.F., Dai, Y.P., Liu, Y.Q., 2014. Thermodynamic analysis of a low-temperature waste heat recovery system based on the concept of solar chimney. Energy Convers. Manage. 80, 78–86.

Chergui, T., Larbi, S., Bouhdjar, A., 2010. Thermo-hydrodynamic aspect analysis of flows in solar chimney power plants – a case study. Renew. Sustain. Energy Rev. 14, 1410–1418.

Cruger, R., 2011. Threatened Tortoises Slow Down Desert Solar Project, May 15 <http://www.treehugger.com/solar-technology/threatened-tortoises-slow-down-desert-solar-project.html>.

Dai, Y.J., Huang, H.B., Wang, R.Z., 2003. Case study of solar chimney power plants in Northwestern regions of China. Renew. Energy 28, 1295–1304.

Davey, R.C., 2006. Device for generating electricity from solar power. Patent, PCT/AU2007/001151/21-08-2006.

Denantes, F., Bilgen, E., 2006. Counter–rotating turbines for solar chimney power plants. Renew. Energy 31, 1873–1891.

Dhahri, A., Omri, A., 2013. A review of solar chimney power generation technology. Int. J. Eng. Advan. Technol. 2, 1–17.

Duffie, J.A., Beckman, W.A., 2013. Solar Engineering of Thermal Processes, forth ed. Wiley Interscience, New York.

Evans, N., 2011. Dallas Dempster's Sky-High Comeback, December 31 <http://www.perthnow.com.au/archive/business/dallas-dempsters-sky-high-comeback/story-e6frg2qu-1226233935573>.

Fasel, H.F., Meng, F.L., Shams, E., Gross, A., 2013. CFD analysis for solar chimney power plants. Sol. Energy 98, 12–22.

Ferreira, A.G., Maia, C.B., Valle, R.M., Cortez, M.F.B., 2006. Balanço energético de uma chaminé solar. Ciência Engenharia 15, 37–43.

Ferreira, A.G., Maia, C.B., Cortez, M.F.B., Valle, R.M., 2008. Technical feasibility assessment of a solar chimney for food drying. Sol. Energy 82, 198–205.

Fluri, T.P., von Backström, T.W., 2008a. Comparison of modelling approaches and layouts for solar chimney turbines. Sol. Energy 82, 239–246.

Fluri, T.P., von Backström, T.W., 2008b. Performance analysis of the power conversion unit of a solar chimney power plant. Sol. Energy 82, 999–1008.

Fluri, T.P., Pretorius, J.P., van Dyk, C., von Backström, T.W., Kröger, D.G., van Zijl, G.P.A.G., 2009. Cost analysis of solar chimney power plants. Sol. Energy 83, 246–256.

Gannon, A.J., von Backström, T.W., 2000. Solar chimney cycle analysis with system loss and solar collector performance. J. Solar Energy Eng. – Trans. ASME 122, 133–137.

Gannon, A.J., von Backström, T.W., 2003. Solar chimney turbine performance. J. Solar Energy Eng. – Trans. ASME 125, 101–106.

Gholamalizadeh, E., Kim, M.-H., 2014. Three-dimensional CFD analysis for simulating the greenhouse effect in solar chimney power plants using a two-band radiation model. Renew. Energy 63, 498–506.

Gholamalizadeh, E., Mansouri, S.H., 2013. A comprehensive approach to design and improve a solar chimney power plant: a special case – Kerman project. Appl. Energy 102, 975–982.

Golder, K., 2003. Combined solar pond and solar chimney. Final year Mechanical Engineering Project. School of Aerospace, Mechanical and Manufacturing Engineering, Bundoora Campus, RMIT University, Melbourne, Australia.

Günther, H., 1931. In hundert Jahren – Die künftige Energieversorgung der Welt (In hundred years – Future energy supply of the world). Kosmos, Franckh'sche Verlagshandlung, Stuttgart.

Guo, P.H., Li, J.Y., Wang, Y., Liu, Y.W., 2013. Numerical analysis of the optimal turbine pressure drop ratio in a solar chimney power plant. Sol. Energy 98, 42–48.

Guo, P.H., Li, J.Y., Wang, Y., 2014. Numerical simulations of solar chimney power plant with radiation model. Renew. Energy 62, 24–30.

Haaf, W., 1984. Solar chimneys, part II: preliminary test results from the Manzanares pilot plant. Int. J. Solar Energy 2, 141–161.

Haaf, W., Friedrich, K., Mayr, G., Schlaich, J., 1983. Solar chimneys, part I: principle and construction of the pilot plant in Manzanares. Int. J. Solar Energy 2, 3–20.

Harte, R., Graffmann, M., Krätzig, W.B., 2012. Optimization of solar updraft chimneys by nonlinear response analysis. In: Zhou, X.P. (Ed.), Proceedings of the 3rd International Conference on Solar Updraft Tower Power Technology. Wuhan, China, pp. 193–202.

Harte, R., Höffer, R., Krätzig, W.B., Mark, P., Niemann, H.-J., 2013. Solar updraft power plants: Engineering structures for sustainable energy generation. Eng. Struct. 56, 1698–1706.

Hartung, C., Marschetzky, H., Link, T., Bauer, M., Künzel, M., Ellwanger, M., Thanh, T.P., Dang, L.N., 2008. (Supervisors: Ruth, J., Gumpp, R.). Solar power plant 2008 <http://www.archineering.de>.

Hedderwick, R.A., 2001. Performance evaluation of a solar chimney power plant. M.Sc.Eng. thesis, University of Stellenbosch, Stellenbosch, South Africa.

Herrick, G., 2013. A Model Solar Updraft Tower Power Plant, February 21 <http://www.wxedge.com/articles/20130220a_model_solar_updraft_tower_power_plant>.

Höffer, R., Wevers, C., Görnandt, V., 2010. Transport and deposition of dust on the collector surface. In: Proceedings of the 2nd International Conference on Solar Chimney Power Technology. Bochum, Germany, pp. 325–338.

Höffer, R., Niemann, H.-J., Wevers, C., 2012. Wind speeds at larger heights and wind driven particle transport on the collector roof. In: Zhou, X.P. (Ed.), Proceedings of the 3rd International Conference on Solar Updraft Tower Power Technology. Wuhan, China, p. 217.

Hummel, M., 2010. Can power from updraft and GreenTowers already compete against conventional technologies? A profitability and risk analysis. In: Proceedings of the 2nd International Conference on Solar Chimney Power Technology. Bochum, Germany, pp. 355–360.

Hurtado, F.J., Kaiser, A.S., Zamora, B., 2012. Evaluation of the influence of soil thermal inertia on the performance of a solar chimney power plant. Energy 47, 213–224.

Islamuddin, A., Al-Kayiem, H.H., Gilani, S.I., 2013. Simulation of solar chimney power plant with an external heat source. In: Proceedings of the 4th International Conference on Energy and Environment. Putrajaya, Malaysia.

Kalash, S., Naimeh, W., Ajib, S., 2013. Experimental investigation of the solar collector temperature field of a sloped solar updraft power plant prototype. Sol. Energy 98, 70–77.

Kasaeian, A.B., Heidari, E., Vatan, S.N., 2011. Experimental investigation of climatic effects on the efficiency of a solar chimney pilot power plant. Renew. Sustain. Energy Rev. 15, 5202–5206.

Kasaeian, A., Ghalamchi, M., Ghalamchi, M., 2014. Simulation and optimization of geometric parameters of a solar chimney in Tehran. Energy Convers. Manage. 83, 28–34.

Kashiwa, B.A., Kashiwa, C.B., 2008. The solar cyclone: a solar chimney for harvesting atmospheric water. Energy 33, 331–339.

Khoo, I., Khor, A., Lee, H.-W., 2011. Solar Chimney for Desalination. Final Report of Project 1061. The University of Adelaide, Adelaide, Australia.

Koonsrisuk, A., 2009. Analysis of flow in solar chimney for an optimal design purpose. Ph.D. thesis, Suranaree University of Technology, Nakhon Ratchasima, Thailand.

Koonsrisuk, A., 2012. Mathematical modeling of sloped solar chimney power plants. Energy 47, 582–589.

Koonsrisuk, A., 2013. Comparison of conventional solar chimney power plants and sloped solar chimney power plants using second law analysis. Sol. Energy 98, 78–84.

Koonsrisuk, A., Chitsomboon, T., 2007. Dynamic similarity in solar chimney modeling. Sol. Energy 81, 1439–1446.

Koonsrisuk, A., Chitsomboon, T., 2009a. Accuracy of theoretical models in the prediction of solar chimney performance. Sol. Energy 83, 1764–1771.

Koonsrisuk, A., Chitsomboon, T., 2009b. A single dimensionless variable for solar chimney power plant modeling. Sol. Energy 83, 2136–2143.

Koonsrisuk, A., Chitsomboon, T., 2010. Theoretical turbine power yield in solar chimney power plants. In: Proceedings of the 3rd International conference on Thermal Issues in Emerging Technologies Theory and Applications. Cairo, Egypt, pp. 339–346.

Koonsrisuk, A., Chitsomboon, T., 2013a. Mathematical modeling of solar chimney power plants. Energy 51, 314–322.

Koonsrisuk, A., Chitsomboon, T., 2013b. Effects of flow area changes on the potential of solar chimney power plants. Energy 51, 400–406.

Koonsrisuk, A., Lorente, S., Bejan, A., 2010. Constructal solar chimney configuration. Int. J. Heat Mass Transf. 53, 327–333.

Koyun, V.A., 2006. Güneş Bacası İle Enerji Üretiminin İncelenmesi. S.D.Ü. Fen Bilimleri Enstitüsü, Doktora Tezi, Isparta, Turkey.

Please cite this article in press as: Zhou, X., Xu, Y. Solar updraft tower power generation. Sol. Energy (2014), http://dx.doi.org/10.1016/j.solener.2014.06.029

Krätzig, W.B., 2013. Physics, computer simulation and optimization of thermo-fluidmechanical processes of solar updraft power plants. Sol. Energy 98, 2–11.

Krätzig, W.B., Harte, R., Montag, U., Wörmann, R., 2009. From large natural draft cooling tower shells to chimneys of solar upwind power plants. In: Proceedings of the International Association for Shell and Spatial Structures Symposium 2009. Valencia, Spain.

Kreetz, H., 1997. Theoretische Untersuchungen und Auslegung eines temporaren Wasserspeichers fur das Aufwindkraftwerk. Diplomarbeit. Energie und Verfahrenstechnik der TU Berlin, Berlin.

Krisst, R.J.K., 1983. Energy transfer system. Alt. Sour. Energy 63, 8–11.

Kröger, D.G., Blaine, D., 1999. Analysis of the driving potential of a solar chimney power plant. Res. Develop. J. South African Inst. Mech. Eng. 15, 85–94.

Kröger, D.G., Buys, J.D., 1999. Radial flow boundary layer development analysis. Res. Develop. J. South African Inst. Mech. Eng. 15, 95–102.

Kröger, D.G., Buys, J.D., 2001. Performance evaluation of a solar chimney power plant. ISES 2001. Solar World Congress, Adelaide, Australia.

Kröger, D.G., Buys, J.D., 2002. Solar chimney power plant performance characteristics. Res. Develop. J. South African Inst. Mech. Eng. 18, 31–36.

Kuck, J., Ziller, C., Schnatbaum-Laumann, L., Gladen, H., 2010. Methodical approach to design the solar collector of a solar chimney power plant. In: Proceedings of the 2nd International Conference on Solar Chimney Power Technology. Bochum, Germany, pp. 293–300.

Kulunk, H., 1985. A prototype solar convection chimney operated under Izmit conditions. In: Proceedings of the 7th Miami International Conference on Alternative Energy Sources. Miami Beach, Florida.

Larbi, S., Bouhdjar, A., Chergui, T., 2010. Performance analysis of a solar chimney power plant in the southwestern region of Algeria. Renew. Sustain. Energy Rev. 14, 470–477.

Lautenschlager, H., Haaf, W., Schlaich, J., 1984. New results from the solar chimney prototype and conclusions for large power plants. In: Proceedings of the European Wind Energy Conference. Hamburg, Germany, pp. 231–235.

Ley, W., 1954. Engineers' Dreams. Viking Press.

Li, J.Y., Guo, P.H., Wang, Y., 2012a. Preliminary investigation of a novel solar and wind energy extraction system. Proc. Inst. Mech. Eng. Part A – J. Power Energy 226, 73–85.

Li, J.Y., Guo, P.H., Wang, Y., 2012b. Effects of collector radius and chimney height on power output of a solar chimney power plant with turbines. Renew. Energy 47, 21–28.

Li, W.B., Wei, P., Zhou, X.P., 2014. A cost-benefit analysis of power generation from commercial reinforced concrete solar chimney power plant. Energy Convers. Manage. 79, 104–113.

Lodhi, M.A.K., 1999. Application of helio–aero–gravity concept in producing energy and suppressing pollution. Energy Convers. Manage. 40, 407–421.

Lorente, S., Koonsrisuk, A., Bejan, A., 2010. Constructal distribution of solar chimney power plants: few large and many small. Int. J. Green Energy 7, 577–592.

Lucier, RE., 1978. Utilization of solar energy. Canada Patent, no. 1023564.

Lucier, RE., 1979a. Apparatus for converting solar to electrical energy. Australia Patent, no. 499934.

Lucier, RE., 1979b. System and apparatus for converting solar heat to electrical energy. Israel Patent, no. 50721.

Lucier, RE., 1981. System for converting solar heat to electrical energy. US Patent, no. 4275309.

Maia, C.B., Ferreira, A.G., Valle, R.M., Cortez, M.F.B., 2009a. Theoretical evaluation of the influence of geometric parameters and materials on the behavior of the airflow in a solar chimney. Comput. Fluids 38, 625–636.

Maia, C.B., Ferreira, A.G., Valle, R.M., Cortez, M.F.B., 2009b. Analysis of the airflow in a prototype of a solar chimney dryer. Heat Transf. Eng. 30, 393–399.

Manon, U., Maxime, R., Boris, L., Mathias, L., 2011. Cheminee tour solaire. Project 1112 on Année universitaire, Université de Pau et des Pays de l'Adour, Pau, France <http://iutpa.univ-pau.fr/live/digitalAssets/103/103388_1112-CHEMINEE_TOUR_SOLAIRE.pdf>.

Mehla, N., Makade, R., Thakur, N.S., 2011. Experimental analysis of a velocity field using variable chimney diameter for solar updraft tower. Int. J. Eng. Sci. Technol. 3, 3167–3171.

Meng, F., Gross, A., Fasel, H.F., 2013. Computational fluid dynamics investigation of solar chimney power plant. In: The 43rd Fluid Dynamics Conference. San Diego, California.

Ming, T.Z., Liu, W., Pan, Y., Xu, G.L., 2008a. Numerical analysis of flow and heat transfer characteristics in solar chimney power plants with energy storage layer. Energy Convers. Manage. 49, 2872–2879.

Ming, T.Z., Liu, W., Xu, G.L., Xiong, Y.B., Guan, X.H., Pan, Y., 2008b. Numerical simulation of the solar chimney power plant systems coupled with turbine. Renew. Energy 33, 897–905.

Ming, T.Z., Wang, X.J., de Richter, R.K., Liu, W., Wu, T.H., Pan, Y., 2012. Numerical analysis on the influence of ambient crosswind on the performance of solar updraft power plant system. Renew. Sustain. Energy Rev. 16, 5567–5583.

Ming, T.Z., de Richter, R.K., Meng, F.L., Pan, Y., Liu, W., 2013a. Chimney shape numerical study for solar chimney power generating systems. Int. J. Energy Res. 37, 310–322.

Ming, T.Z., Gui, J.L., de Richter, R.K., Pan, Y., Xu, G.L., 2013b. Numerical analysis on the solar updraft power plant system with a blockage. Sol. Energy 98, 58–69.

Ming, T.Z., Meng, F.L., Liu, W., Pan, Y., de Richter, R.K., 2013c. Analysis of output power smoothing method of the solar chimney power generating system. Int. J. Energy Res. 37, 1657–1668.

Mohammad, O.H., Obada, R., 2012. Experimental solar chimney data with analytical model prediction. In: World Renewable Energy Forum. Denver, Colorado.

Motsamai, O., Bafetanye, L., Mashaba, K., Kgaswane, O., 2013. Experimental investigation of solar chimney power plant. J. Energy Power Eng. 7, 1980–1984.

Mullett, L.B., 1987. The solar chimney overall efficiency, design and performance. Int. J. Ambient Energy 8, 35–40.

Najmi, M., Nazari, A., Mansouri, H., Zahedi, G., 2012. Feasibility study on optimization of a typical solar chimney power plant. Heat Mass Transf. 48, 475–485.

NASA Earth Observations, 2014. Land Cover Classification (1 year) <http://neo.sci.gsfc.nasa.gov/view.php?datasetId=MCD12C1_T1> (retrieved on January 25).

NASA SSE, 2014. NASA Surface Meteorology and Solar Energy: Global Data Sets <https://eosweb.larc.nasa.gov/cgi-bin/sse/global.cgi?email=skip@larc.nasa.gov> (retrieved on January 25).

Niemann, H.-J., Lupi, F., Höffer, R., Hubert, W., Borri, C., 2009. The solar updraft power plant: Design and optimization of the tower for wind effects. In: Proceedings of the 5th European & African Conference on Wind Engineering. Florence, Italy.

Ninic, N., 2006. Available energy of the air in solar chimneys and the possibility of its ground–level concentration. Sol. Energy 80, 804–811.

Niroomand, N., Amidpour, M., 2013. New combination of solar chimney for power generation and seawater desalination. Desalin. Water Treat. 51, 7401–7411.

Nizetic, S., Klarin, B., 2010. A simplified analytical approach for evaluation of the optimal ratio of pressure drop across the turbine in solar chimney power plants. Appl. Energy 87, 587–591.

Nizetic, S., Ninic, N., Klarin, B., 2008. Analysis and feasibility of implementing solar chimney power plants in the Mediterranean region. Energy 33, 1680–1690.

Okoye, C.O., Atikol, U., 2014. A parametric study on the feasibility of solar chimney power plants in North Cyprus conditions. Energy Convers. Manage. 80, 178–187.

Onyango, F.N., Ochieng, R.M., 2006. The potential of solar chimney for application in rural areas of developing countries. Fuel 85, 2561–2566.

Padki, M.M., Sherif, S.A., 1999. On a simple analytical model for solar chimneys. Int. J. Energy Res. 23, 345–349.

Please cite this article in press as: Zhou, X., Xu, Y. Solar updraft tower power generation. Sol. Energy (2014), http://dx.doi.org/10.1016/j.solener.2014.06.029

Palyvos, J.A., 2008. A survey of wind convection coefficient correlations for building envelope energy systems' modeling. Appl. Therm. Eng. 28, 801–808.

Panse, S.V., Jadhav, A.S., Gudekar, A.S., Joshi, J.B., 2011. Inclined solar chimney for power production. Energy Convers. Manage. 52, 3096–3102.

Papageorgiou, C.D., 2003. Floating solar chimney. Patent, PCT/GR03/00037/27-03-2003.

Papageorgiou, C.D., 2004. Optimum design for solar power stations with floating solar chimneys. Proceedings of ISES Asia Pacific Solar Energy Conference. Kwangju, Korea, pp. 763–772.

Papageorgiou, C.D., 2006. Floating solar chimney power stations with thermal storage. In: Proceedings of the IASTED Conference on European Power and Energy Systems. Rhodes, Greece.

Papageorgiou, C.D., 2013. Enclosed Solar Chimney Technology <http://www.gchimneytech.com/technology.html>.

Papageorgiou, C.D., Katopodis, P., 2009. A modular solar collector for desert floating solar chimney technology. In: Mastorakis, N.E. (Ed.), Energy, Environment, Ecosystems, Development and Landscape Architecture. WSEAS Press, Athens, Greece, pp. 126–132.

Pastohr, H., Kornadt, O., Gurlebeck, K., 2004. Numerical and analytical calculations of the temperature and flow field in the upwind power plant. Int. J. Energy Res. 28, 495–510.

Pasumarthi, N., Sherif, S.A., 1998a. Experimental and theoretical performance of a demonstration solar chimney model – Part I: mathematical model development. Int. J. Energy Res. 22, 277–288.

Pasumarthi, N., Sherif, S.A., 1998b. Experimental and theoretical performance of a demonstration solar chimney model – Part II: experimental and theoretical results and economic analysis. Int. J. Energy Res. 22, 443–461.

Patel, S.K., Prasad, D., Ahmed, M.R., 2014. Computational studies on the effect of geometric parameters on the performance of a solar chimney power plant. Energy Convers. Manage. 77, 424–431.

Petela, R., 2009. Thermodynamic study of a simplified model of the solar chimney power plant. Sol. Energy 83, 94–107.

Pretorius, J.P., 2004. Solar tower power plant performance characteristics. M.Sc.Eng. thesis, University of Stellenbosch, Stellenbosch, South Africa.

Pretorius, J.P., 2007. Optimization and control of a large–scale solar chimney power plant. Ph.D. thesis, University of Stellenbosch, Stellenbosch, South Africa.

Pretorius, J.P., Kröger, D.G., 2006a. Critical evaluation of solar chimney power plant performance. Sol. Energy 80, 535–544.

Pretorius, J.P., Kröger, D.G., 2006b. Solar chimney power plant performance. J. Solar Energy Eng. – Trans. ASME 128, 302–311.

Pretorius, J.P., Kröger, D.G., 2007. Sensitivity analysis of the operating and technical specifications of a solar chimney power plant. J. Solar Energy Eng. – Trans. ASME 129, 171–178.

Pretorius, J.P., Kröger, D.G., 2009. The influence of environment on solar chimney power plant performance. Res. Develop. J. South African Inst. Mech. Eng. 25, 1–9.

Putkaradze, V., Vorobieff, P., Mammoli, A., Fathi, N., 2013. Inflatable free-standing flexible solar towers. Sol. Energy 98, 85–98.

Qin, P., 2013. Investigation into static and dynamic response of solar chimney under different kinds of loads. Master thesis, Huazhong University of Science and Technology, Wuhan, China.

Raney, S.M., Brooks, J.R., Schaffer, J.P., French, J.J., 2012. Experimental validation of solar chimney performance models and operational characteristics for small scale remote applications. In: Proceedings of the ASME 2012 6th International Conference on Energy Sustainability. San Diego, California, pp. 27–32.

Sangi, R., 2012. Performance evaluation of solar chimney power plants in Iran. Renew. Sustain. Energy Rev. 16, 704–710.

Sangi, R., Amidpour, M., Hosseinizadeh, B., 2011. Modeling and numerical simulation of solar chimney power plants. Sol. Energy 5, 829–838.

Schlaich, J., 1995. The Solar Chimney: Electricity From the Sun. Edition Axel Menges, Stuttgart, Germany.

Schlaich, J., 1999. Tension structures for solar electricity generation. Eng. Struct. 21, 658–668.

Schlaich, J., Bergermann, R., Schiel, W., Weinrebe, G., 2004. Sustainable electricity generation with solar updraft towers. Struct. Eng. Int. 14, 225–229.

Schlaich, J., Bergermann, R., Schiel, W., Weinrebe, G., 2005. Design of commercial solar updraft tower systems – utilization of solar induced convective flows for power generation. J. Solar Energy Eng. – Trans. ASME 127, 117–124.

Senanayake, D., 1996. Chimney. US Patent, no. 5527216.

Serag-Eldin, M.A., 2004a. Mitigating adverse wind effects on flow in solar chimney plants. In: Proceedings of the 4th International Engineering Conference. Sharm El Sheikh, Egypt.

Serag-Eldin, M.A., 2004b. Computing flow in a solar chimney plant subject to atmospheric winds. In: Proceedings of 2004 ASME Heat Transfer/Fluids Engineering Summer Conference. Charlotte, North Carolina.

Sharples, S., Charlesworth, P.S., 1998. Full-scale measurements of wind-induced convective heat transfer from a roof-mounted flat plate solar collector. Sol. Energy 62, 69–77.

Spencer, R.W., 2013. Update on EnviroMission's Arizona Solar Tower Project, June 27 <http://www.drroyspencer.com/2013/06/update-on-enviromissions-arizona-solar-tower-project>.

Stamatov, V., 2010. Utilisation of solar updraft towers for electricity generation and improvement of air quality near closed landfills in Australia. In: 2009 Annual Bulletin of the Australian Institute of High Energetic Materials, vol. 1, pp. 1–14.

Stinnes, W.-W., 2010. Humus as the backbone of GreenTower revenues – green revolution in agriculture, soil rehabilitation, forestry, desert cultivation and CO_2 sequestration. In: Proceedings of the 2nd International Conference on Solar Chimney Power Technology. Bochum, Germany, pp. 345–354.

Thomashausen, A., 2010. GreenTower in world politics – how it solves shortages in power, fuel, food and water and reduces conflict potentials. In: Proceedings of the 2nd International Conference on Solar Chimney Power Technology. Bochum, Germany, pp. 339–344.

Üçgül, İ., Koyun, V.A., 2010. Güneş Bacası Tasarım Parametreleri ve Performansının Deneysel Olarak İncelenmesi (Experimental investigations on performance and design parameters of solar chimney). Pamukkale Univ. J. Eng. Sci. 16, 255–264.

VanReken, T.M., Nenes, A., 2009. Cloud formation in the plumes of solar chimney power generation facilities: a modeling study. J. Solar Energy Eng. – Trans. ASME 131, 011009.

Von Backström, T.W., 2003. Calculation of pressure and density in solar power plant chimneys. J. Solar Energy Eng. – Trans. ASME 125, 127–129.

Von Backström, T.W., Fluri, T.P., 2006. Maximum fluid power condition in solar chimney power plants – an analytical approach. Sol. Energy 80, 1417–1423.

Von Backström, T.W., Gannon, A.J., 2000a. Compressible flow through solar power plant chimneys. J. Solar Energy Eng. – Trans. ASME 122, 138–145.

Von Backström, T.W., Gannon, A.J., 2000b. The solar chimney air standard thermodynamic cycle. Res. Develop. J. South African Inst. Mech. Eng. 16, 16–24.

Von Backström, T.W., Gannon, A.J., 2004. Solar chimney turbine characteristics. Sol. Energy 76, 235–241.

Von Backström, T.W., Bernhardt, A., Gannon, A.J., 2003. Pressure drop in solar power plant chimneys. J. Solar Energy Eng. – Trans. ASME 125, 165–169.

Von Backström, T.W., Harte, R., Höffer, R., Krätzig, W.B., Kröger, D.G., Niemann, H.-J., van Zijl, G.P.A.G., 2008. State and recent advances in research and design of solar chimney power plant technology. VGB PowerTech J. PT07 10, 64–71.

Watmuff, J.H., Charters, W.W.S., Proctor, D., 1977. Solar and wind induced external coefficients – solar collectors. Cooperation Mediterraneenne pour l'Energie Solaire, Revue Internationale d'Heliotechnique, 2nd Quarter, 56.

Please cite this article in press as: Zhou, X., Xu, Y. Solar updraft tower power generation. Sol. Energy (2014), http://dx.doi.org/10.1016/j.solener.2014.06.029

Wei, Y.L., Wu, Z.K., 2012. Shed absorbability and tower structure characteristics of the solar heated wind updraft tower power. In: Zhou, X.P. (Ed.), Proceedings of the 3rd International Conference on Solar Updraft Tower Power Technology. Wuhan, China, pp. 26–34.

Wesoff, E., 2011. EnviroMission Wins $29.8 M In Debt/Equity for Solar Updraft Tower, January 13 <http://www.greentechmedia.com/articles/read/enviromission-secures-30m-hybrid-debt-equity-facility>.

Wikipedia, 2014. Solar Updraft Tower <http://en.wikipedia.org/wiki/Solar_updraft_tower> (retrieved on January 25).

Xu, G.L., Ming, T.Z., Pan, Y., Meng, F.L., Zhou, C., 2011. Numerical analysis on the performance of solar chimney power plant system. Energy Convers. Manage. 52, 876–883.

Xu, H.T., Karimi, F., Yang, M., 2014. Numerical investigation of thermal characteristics in a solar chimney project. J. Solar Energy Eng. – Trans. ASME 136, 011008.

Zandian, A., Ashjaee, M., 2013. The thermal efficiency improvement of a steam Rankine cycle by innovative design of a hybrid cooling tower and a solar chimney concept. Renew. Energy 51, 465–473.

Zheng, Y., Ming, T.Z., Zhou, Z., Yu, X.F., Wang, H.Y., Pan, Y., Liu, W., 2010. Unsteady numerical simulation of solar chimney power plant system with energy storage layer. J. Energy Inst. 83, 86–92.

Zhou, X.P., Yang, J.K., 2009. A novel solar thermal power plant with floating chimney stiffened onto a mountainside and potential of the power generation in China's deserts. Heat Transf. Eng. 30, 400–407.

Zhou, X.P., Yang, J.K., Xiao, B., Hou, G.X., 2007a. Experimental study of the temperature field in a solar chimney power setup. Appl. Therm. Eng. 27, 2044–2050.

Zhou, X.P., Yang, J.K., Xiao, B., Hou, G.X., 2007b. Simulation of a pilot solar chimney power equipment. Renew. Energy 32, 1637–1644.

Zhou, X.P., Yang, J.K., Xiao, B., Hou, G.X., Shi, X.Y., 2008. Special climate around a commercial solar chimney power plant. J. Energy Eng. – Trans. ASCE 134, 6–14.

Zhou, X.P., Yang, J.K., Ochieng, R.M., Xiao, B., 2009a. Numerical investigation of a plume from a power generating solar chimney in an atmospheric cross flow. Atmos. Res. 91, 26–35.

Zhou, X.P., Yang, J.K., Wang, F., Xiao, B., 2009b. Economic analysis of floating solar chimney power plant. Renew. Sustain. Energy Rev. 13, 736–749.

Zhou, X.P., Yang, J.K., Wang, J.B., Xiao, B., 2009c. Novel concept for producing energy integrating a solar collector with a man made mountain hollow. Energy Convers. Manage. 50, 847–854.

Zhou, X.P., Yang, J.K., Wang, J.B., Xiao, B., Hou, G.X., Wu, Y.Y., 2009d. Numerical investigation of a compressible flow through a solar chimney. Heat Transf. Eng. 30, 670–676.

Zhou, X.P., Yang, J.K., Xiao, B., Hou, G.X., Xing, F., 2009e. Analysis of chimney height for solar chimney power plant. Appl. Therm. Eng. 29, 178–185.

Zhou, X.P., Yang, J.K., Xiao, B., Li, J., 2009f. Night operation of solar chimney power system using solar ponds for heat storage. Int. J. Global Energy Issues 31, 193–207.

Zhou, X.P., Wang, F., Fan, J., Ochieng, R.M., 2010a. Performance of solar chimney power plant in Qinghai–Tibet Plateau. Renew. Sustain. Energy Rev. 14, 2249–2255.

Zhou, X.P., Wang, F., Ochieng, R.M., 2010b. A review on solar chimney power technology. Renew. Sustain. Energy Rev. 14, 2315–2338.

Zhou, X.P., Xiao, B., Liu, W.C., Guo, X.J., Yang, J.K., Fan, J., 2010c. Comparison of classical solar chimney power system and combined solar chimney system for power generation and seawater desalination. Desalination 250, 249–256.

Zhou, X.P., Bernardes, M.A.d.S., Ochieng, R.M., 2012. Influence of atmospheric cross flow on solar updraft tower inflow. Energy 42, 393–400.

Zhou, X.P., Qin, P., Liu, C., Qian, C.Q., 2013a. Wind channel installed at the chimney outlet for enhancing ventilation effect. Chinese Patent, no. ZL2012203055549.

Zhou, X.P., Qin, P., Zheng, H.M., Liu, C., Qian, C.Q., 2013b. A greenhouse equipment (solar collector) with auto-movable roof and application. Chinese Patent, no. ZL2012101347814.

Zhou, X.P., von Backström, T.W., Bernardes, M.A.d.S., 2013c. Introduction to the special issue on solar chimneys. Sol. Energy 98, 1.

Zhou, X.P., Yuan, S., Bernardes, M.A.d.S., 2013d. Sloped-collector solar updraft tower power plant performance. Int. J. Heat Mass Transf. 66, 798–807.

Zhou, X.P., Xu, Y.Y., Yuan, S., Chen, R.C., Song, B., 2014. Pressure and power potential of sloped-collector solar updraft tower power plant. Int. J. Heat Mass Transf. 75, 450–461.

Zongker, J.D., 2013. Life cycle assessment of solar updraft tower power plant: EROEI and GWP as a design tool. M.Sc. Eng. thesis, Wichita State University, Wichita, Kansas.

Zou, Z., Guan, Z.Q., Gurgenci, H., Lu, Y.S., 2012. Solar enhanced natural draft dry cooling tower for geothermal power applications. Sol. Energy 86, 2686–2694.

Zou, Z., Guan, Z.Q., Gurgenci, H., 2013. Optimization design of solar enhanced natural draft dry cooling tower. Energy Convers. Manage. 76, 945–955.

Zou, Z., Guan, Z.Q., Gurgenci, H., 2014. Numerical simulation of solar enhanced natural draft dry cooling tower. Sol. Energy 101, 8–18.

Zuo, L., Zheng, Y., Li, Z.J., Sha, Y.J., 2011. Solar chimneys integrated with sea water desalination. Desalination 76, 207–213.

Zuo, L., Yuan, Y., Li, Z.J., Zheng, Y., 2012. Experimental research on solar chimneys integrated with seawater desalination under practical weather condition. Desalination 298, 22–33.

Please cite this article in press as: Zhou, X., Xu, Y. Solar updraft tower power generation. Sol. Energy (2014), http://dx.doi.org/10.1016/j.solener.2014.06.029